MR. BRIAN DILLON GRIEVE (Orcid ID : 0000-0001-7278-8632)



Article type : Original Article

**Title**

Modeling the impacts of climate change on thorny skate (*Amblyraja radiata*) on the Northeast US shelf using trawl and longline surveys

**Running Title**

Climate change and thorny skate

**Authors**

Brian Dillon Grieve[1,2*+], Jonathan A Hare[3], W. David McElroy[1,3]

[1] Integrated Statistics
Woods Hole, Massachusetts, United States

[2] NOAA Northeast Fisheries Science Center
Narragansett, Rhode Island, United States

[3] NOAA Northeast Fisheries Science Center
Woods Hole, Massachusetts United States

[*] Present Address

The Nature Conservancy
Narragansett, Rhode Island, United States

+ Corresponding author, grievebr@gmail.com

**Keywords**
Thorny skate, climate change, conservation, fisheries, longline, bottom trawl, GAM

**Acknowledgements**

We thank Vincent Saba of NMFS for providing the GFDL CM 2.6 climate model. We thank all the officers and crew of the NOAA *FR/V H.B. Bigelow* and the scientific staff of the Ecosystems Surveys Branch of the NEFSC. We thank the captains and crews of the *F/V Mary Elizabeth* and *F/V Tenacious II*, and the scientific staff of the Cooperative Research Branch of the NEFSC. We acknowledge the World Climate Research Programme's Working Group on Coupled Modelling, which is responsible for CMIP, and we thank the climate modeling groups (Table 2) for producing and making available their model output. Acknowledgment of the above individuals does not imply their endorsement of this work; the authors have sole responsibility for the content of this contribution. Funding was provided by the NOAA Fisheries Office of Science and Technology. The views expressed herein are those of the authors and do not necessarily reflect the views of NOAA or any of its subagencies.

**Conflicts of Interest**

The authors have no conflicts of interest in relation to the present work

**Data Availability Statement**

The code that support the findings of this study are available from the corresponding author's GitHub repository (github.com/grievebr/thornyskate). Data can be obtained from corresponding author by reasonable request.

**Funding Source**

NOAA Fisheries Office of Science and Technology

**Abstract**

Climate change has been shown to impact marine fish populations and communities. With small population sizes, long reproduction times, and a rapidly warming habitat, thorny skate (*Amblyraja radiata*) could be particularly vulnerable. To examine this possibility, we used a two-stage generalized additive model to project future thorny skate abundances under two different climate scenarios. This is the first study in the northeastern United States to compare projections based on different survey methods (bottom trawl and longline) and results were heavily impacted by survey methodology. Models trained with the NOAA Bottom Trawl Survey projected a decrease in abundance of ~60-80% in the Gulf of Maine and Georges Bank under the RCP 8.5 climate scenario. With aggressive mitigation (RCP 4.5), these decreases could be reduced to ~35-45%. Models trained with a recent NOAA longline survey indicated that thorny skate abundance would be reduced 22% and 37% under business-as-usual and mitigation, respectively. There are substantial methodological differences between the two datasets, including capture technique and efficiency, total habitat coverage, and spatiotemporal coverage. This underscores the importance of continued, methodologically-diverse surveys on the Northeast US continental shelf. Our results indicate that climate change will continue to negatively impact thorny skate populations by reducing the amount of thermally suitable habitat in the southern extent of their range. This information should be considered in future management decisions.

## Introduction

Global temperatures are expected to continue to rise as a direct effect of anthropogenic greenhouse gases emissions (IPCC 2013). This has many potential effects on the global ocean, including transforming marine communities by altering species abundances and distributions (Hoegh-Guldberg and Bruno 2010; Poloczanska et al. 2013). Such shifts have already been associated with climate change (Parmesan and Yohe 2003; Perry 2005), and many more are

expected in the future (Cheung et al. 2010; Kleisner et al. 2017; Morley et al. 2018). For example, the Gulf of Maine (GOM) has warmed faster than 99.9% of the global ocean (Pershing et al. 2015), and the northeastern US has seen changes in both species distributions and community structure (Friedland and Hare 2007; Nye et al. 2009; Bell et al. 2015).

Thorny skate *Amblyraja radiata* (Donovan, 1808) are a slow-growing, broadly-carnivorous demersal elasmobranch (Packer, Zetlin, and Vitaliano 2003; Sosebee 2005). It was once the most abundant skate species in the GOM (McEachran and Musick 1975), and its population in the Northwest Atlantic continues along the Scotian Shelf up to the Gulf of Saint Lawrence and into boreal distributions across the Atlantic (Scott and Scott 1988). To the south, thorny skate are occasionally but infrequently found on Georges Bank (GB) and southern New England (Figure 1; Sosebee et al. 2016). They have been seen at a broad range of temperatures and depth (McEachran and Musick 1975; Kneebone et al. 2020), and tagging studies have indicated little movement from initial capture sites (Templeman 1984; Kneebone et al. 2020). For a map of some of these and other locations, see Brillant et al (2015).

According to the National Oceanic and Atmospheric Administration (NOAA) Northeast Fisheries Science Center (NEFSC) bottom trawl surveys, thorny skate populations in the GOM have sharply declined in the last 50 years (Sosebee et al. 2016). Biomass has decreased from 5.6 kg/tow in the 1970s to 0.17 kg/tow from 2013-2015, less than 5% of its historical peak (Sosebee et al. 2016). They continue to occupy less area, with small changes in distribution towards deeper and slightly more southern waters (Nye et al. 2009). Much of this decline is thought to be related to fishing, and the possession of the species in U.S. waters has been prohibited since 2003 (New England Fishery Management Council 2003). Barndoor skate (*Dipturus laevis*) were also prohibited after steep population declines, but unlike thorny skate, have since shown adequate recovery to re-permit some commercial harvest (NMFS 2018). There are many potential reasons the two species have not recovered equally, such as different demography and life history or movement capabilities, reliance on different habitats and communities, differing levels of incidental catch, or perhaps have been differently impacted by existing climate change.

Due to these population declines and the high vulnerability of thorny skate to climate change (Hare et al. 2016; Kleisner et al. 2017; Shackell, Ricard, and Stortini 2014), the National Marine Fisheries Service (NMFS) was twice petitioned to list thorny skate as threatened or

endangered under the Endangered Species Act (Federal Register 2015, 2017; NMFS 2017). Important considerations for threatened status relevant here include current fish populations in relation to historical abundance, trends in abundance, and natural and human influenced factors that cause variability in survival and abundance (ESA sec. 4(a)(1)). In 2017, NMFS determined that thorny skate are not likely to become extinct in a large portion of its range in the foreseeable future and concluded that an ESA listing was unwarranted at the time (NMFS 2017).

Thorny skate are infrequently encountered and generally prefer specific structured bottom habitat (NMFS 2017; Sosebee et al. 2016). As such, trawling may be an inefficient method to fully represent thorny skate abundance in an area. Trawling is both unable to sample complex habitats and has a low capture efficiency of thorny skate (0.1 Edwards 1968) due to the skate being able to avoid capture beneath the trawl. This can lead to a bias in biomass projections (Davies and Jonsen 2011), however if capture efficiency has been standardized, the trawl survey can still be useful to recognize a trend. To address the potential role of habitat in low capture efficiency, the NEFSC Cooperative Research Branch has conducted a pilot longline survey in the GOM since 2014 (McElroy et al. 2019). Due to the differences in their respective capture methodologies and targeted habitats, the two surveys cannot be expected to project similar total abundance. However, trends of abundance are comparable in the context of examining the effect of climate change in the sampled habitats.

Previous studies have determined that thorny skate are vulnerable to climate change (Hare et al. 2016) and prone to future thermal habitat shortage (Kleisner et al. 2017; Shackell et al. 2014), yet do not offer the species-specific precision that future ESA decisions require. This investigation aims to offer a more thorough analysis of climate threats to thorny skate on the Northeast United States Continental Shelf. First, we utilize a two-step delta-generalized additive model (GAM) and specific climate scenarios to project the likelihood and abundance of thorny skate for the "foreseeable future", which in this case is 40 years from the initial ESA petition (NMFS 2017). Second, we extend this projection to the end of the century, when the impacts of two different climate mitigation scenarios become more prominent. Third, we create a similar GAM trained with samples from a pilot longline survey to examine how sampling methodology impacts our abundance projections.

## Methods

We used a statistical model trained with current physical conditions and observations to predict thorny skate catch per unit effort (CPUE) with future physical conditions for two time periods: the "foreseeable future" defined in the potential ESA listing (2046-2065, hereafter "2055 period") and a longer-term outlook in 2081-2100 ("2100 period"). This required four different steps: 1) Gathering thorny skate observations and the physical conditions they were sampled at, 2) acquiring static benthic habitat descriptors and dynamic climate model output, 3) creating a statistical model to establish a relationship between thorny skate and predictor variables, and 4) combining those data and models to create future projections.

### 1. Thorny Skate Observations

We used two types of thorny skate catch data to train three different varieties of models. Trawl survey data was obtained from the NOAA NEFSC bottom trawl survey from 1963-2012. The trawl survey covers an area from Cape Hatteras, NC (~35°N) up the continental shelf through all US territorial waters in the GOM. The Scotian Shelf was sampled until 1986. The trawl survey output was presented as CPUE, or the stratified mean number of skate per tow (Sosebee et al. 2016). Depth and bottom-water temperature (BT) were recorded for every tow over the length of the trawl series. Bottom salinity (BS) was added in the fall of 1996. Samples were removed if BT or BS (if applicable) were unavailable. If depth was unavailable for a sample, ETOPO2, a 2' bathymetric representation of satellite altimetry (National Geophysical Data Center 2006), was used instead.

The NEFSC bottom trawl survey takes place in the spring (usually March-May) and fall (usually September-November), however there have been summer and winter surveys at various times throughout the period (Azarovitz 1981; Azarovitz et al. 1997). The spring and fall surveys show similar capture rates (13.4%-16.6%, respectively), while winter and summer are lower. All surveys were pooled in analysis, but season was included as a categorical variable in the statistical model.

We trained the model with both the full timeseries and a shorter timeseries beginning in the fall of 1996. The longer time series contains more observations and can better convey ideal conditions for thorny skate before the decline in population. The shorter timeseries includes

bottom salinity and primarily contains data from years after the 2003 fishing moratorium, or years where the total abundance is very similar. Although it is expected that this will shift the mean projections of the model, we can compare the magnitude of projected changes from one timeseries model to the other. For any stratum that contained multiple samples on the same day, we averaged the samples into a single observation per strata per cruise, reducing the daily variability of the capture data, which is less important for future abundance trends. Portions of some strata may be smaller than the 0.1° climatology can resolve, but these cases are rare. Strata are mapped in Sosebee et al. (2016).

We also trained a similar model with the three available years (2014-2016) of the NEFSC Northeast Cooperative Research Program bottom longline survey (McElroy et al. 2019). The survey covers an area from just north of Cape Cod stretching approximately 100x200 km north and east through the GOM, specifically targeting complex benthic habitats that could not be easily sampled by trawls (see Sosebee et al. 2016 figure 66). Each observation contained BT and depth at each end of the line (McElroy et al. 2019). The end points of the longline sets were 1 nm apart, so physical variables were matched to a single value at the midpoint of the two ends at set time. Unlike the trawl survey data, longline samples were not aggregated by strata. Additional details for each of these surveys can be found in the appendix.

2. Benthic and Climate Data

To describe skate benthic habitat, three indices of benthic terrain and one sediment classifier were obtained from The Nature Conservancy Northwest Atlantic Marine Ecoregional Assessment (NAMERA; Greene et al. 2010). Terrain variables included the bathymetric position index (BPI), an indicator of elevation related to the surrounding landscape, vector ruggedness measurement (VRM), an estimate of heterogeneity of the landscape, and rugosity, the ratio of surface area to planar area (Hare et al. 2012; Lundblad et al. 2006; Sappington, Longshore, and Thompson 2007). Soft sediment is an estimate of sediment grain size based on the United States Geological Survey East-Coast texture sediment database (McMullen, Paskevich, and Poppe 2014). These variables were taken from a uniform grid and assumed static regardless of climate change. These values were matched to observations at their original resolution (~0.003° – ~0.004°), but then averaged to 0.1° for future projections.

Future BT and BS were included from five separate climate models (GCMs) used in the Intergovernmental Panel on Climate Change Fifth Assessment Report (Table 2) under two climate change scenarios: Representative Concentration Pathway (RCP) 8.5 was designed as a "business as usual" scenario considering trends in greenhouse gas emissions at the time while RCP 4.5 represents a scenario of aggressive mitigation, but without assuming large-scale negative emissions (Moss et al. 2010). RCP scenarios were implemented from 2006 onward, with 1855-2005 considered the historical run. Therefore, 1986-2005 is used as the comparison period for RCP scenarios. Time periods consist of 20-year averages to mitigate interannual variability of ocean cycles. To help account for the coarse resolution of these models (~1.0°), we statistically downscaled each climate model to 0.1° climatologies developed by the World Ocean Atlas (WOA; (Locarnini et al. 2013; Zweng et al. 2013) by adding the difference between the future and present time periods of each climate model to the present period WOA climatology (Grieve, Curchitser, and Rykaczewski 2016; Stock et al. 2011). Statistically downscaled climate models are a useful, however do not capture finer scale oceanographic dynamics that could be differently impacted with climate change. To investigate this possibility, projections were also made with the 0.10° GFDL CM 2.6 model using a transient climate response scenario. This is not the same emissions experiment as RCP scenarios, so was not included in the ensemble, but is included separately in the appendix.

## 3. Statistical Presence and Abundance Models

We utilized two separate GAMs to examine the relationship between thorny skate and its environment in the bottom trawl surveys. GAMs are beneficial because they express relationships as a smoother function instead of a linear family (Wood 2006) and are commonly used to model species presence and abundances (e.g. Guisan, Edwards, and Hastie 2002; Morley et al. 2018). The first model was a GAM utilizing presence-absence (P/A) data from all survey strata to predict a continuous likelihood of occurrence. A binomial distribution was used based on the two-factor response variable. The initial form for each P/A model was:

$$P/A \sim s(BT) + s(BS) + s(depth) + s(BPI) + s(VRM) + s(rugosity) + s(sediment\ size) + season$$

where BT is bottom-water temperature; BS is bottom-water salinity (short timeseries only); sediment size is the grain size of the sediment; BPI, VRM, and rugosity are estimates of benthic complexity; and season is the categorical season the sample was taken in. s is the spline

smoother function. The maximum degrees of freedom for each smoother was set to four, preventing the smoothers from overfitting the data and inferring relationships that may not be biologically relevant.

The second model was a negative binomial GAM trained with the zero-truncated CPUE. We used a negative binomial distribution because CPUE is overdispersed and represented in non-integer values. The initial form for each CPUE model was:

$$CPUE \sim s(BT) + s(BS) + s(depth) + s(BPI) + s(VRM) + s(rugosity) + s(sediment\ size) + season$$

The two-step zero-truncated negative binomial model was not appropriate for the longline data due to differences in catch numbers, capture success rate, and how effort is standardized. Because the catch data did not have excessive zeros and the response was presented as counts, we used a Poisson distribution in the GAM:

$$CPUE \sim s(BT) + s(depth) + s(BPI) + s(VRM) + s(rugosity) + s(sediment\ size)$$

where the response is the catch number of all samples in the longline. Because effort was standardized before the survey (i.e. every line had the same length, number of hooks, and average soak time), effort is 1 and CPUE equals the catch number. We did not include season as a factor in the model because a two-tailed T Test indicated that catch numbers in the spring and fall surveys were not significantly different between seasons ($p = 0.17$).

Each model was trained with every combination of predictor variables, and the model with the minimum Akaike Information Criterion (AIC; Akaike 1974) was selected as the final model. If AIC between two models was close ($\Delta AIC < 2$), other factors such as adjusted $R^2$ and deviance explained were considered. A 70% subset of each skate dataset was used for training, with the remaining 30% withheld for testing. Test statistics include Pearson correlation tests between the withheld observations and combined modeled abundance and area under the curve (AUC) for P/A models.

4. Projected Future Abundances

Responses for all five GAMs were predicted utilizing the 0.1° static habitat variables and dynamic bottom temperature and salinity from each downscaled GCM for every month from 1955-2100 for both RCP scenarios (Table 2). Corresponding zero-truncated abundance

predictions and P/A likelihoods were multiplied together to form one final abundance projection (Lo, Jacobson, and Squire 1992). Although all months were projected by the GCM, results from spring (March-May average) and fall (September-November average) are primarily discussed here because they are more relevant to NEFSC protocols. In places where annual averages are discussed, all months were included for the trawl survey models and spring/fall months for the longline model.

All GAMs were created in R (version 3.4.1, R Core Team 2017) using the 'mgcv' package (Wood 2006). AUC was calculated using the package 'pROC' (Robin et al. 2011). Figures were created in MATLAB (version 2019b; Mathworks Inc 2019) using the open-source m_map software package (https://www.eoas.ubc.ca/~rich/map.html ) for all mapping.

## Results

### Observations

The long timeseries showed greater abundances than the short series, with 1963-1996 averaging 3.19 skate per tow (CPUE) and 1997-2013 averaging 0.54 CPUE in the GOM (Figure 1). Over all mean-stratified samples, fall averaged 2.84 CPUE, while spring averaged 1.91 CPUE. For the longline survey, 58% of the samples had positive catches, averaging 5.88 skate per station overall. These surveys showed a decrease in skate as stations moved eastward over the longline survey area. Unlike the trawl series, there were slightly more skate captured in the spring than the fall, but this result was statistically insignificant.

### Climate Models

By the 2055 period, bottom temperatures in the GOM are projected to warm by 2.39±0.81°C (region mean ± SD) from the 1986-2005 period under RCP 8.5 and 1.87±0.90°C under RCP 4.5 (Figure 2). By the 2100 period, this is expected to increase to 4.16 ± 0.87 °C and 2.43 ±0.95 °C from the 1986-2005 period under RCPs 8.5 and 4.5, respectively (Figure 3). In both scenarios, the warming across the region was reasonably homogeneous. GCMs CanESM and MIROC5 projected more warming across the entire region than the other three models (not shown). Likewise, the same two GCMs projected a greater salinity increase than the ensemble

288 average. By 2100, salinity was projected to increase 0.50 ± 0.29 and 0.33 ± 0.21 under RCPs 8.5
289 and 4.5, respectively (Figure A1).

290 Statistical Models

291 Depth, BT, and sediment size were included in the best-fitting skate model for all five
292 modeling situations, while season and BS were included in all best-fitting modeling situations
293 which those variables were available for (Tables 1; A1-A5). The longline GAM had the most
294 complex model, including all available variables with a significance of $p<0.001$. The short and
295 long bottom-trawl presence-absence models explained 53% and 56% of the deviance,
296 respectively, and had an AUC of 0.95 and 0.94. The CPUE bottom trawl models explained 21%
297 and 14% of the deviance for positive tows. After the models were combined, they had
298 Spearman's correlation coefficients of 0.56 and 0.64, respectively, with the test set. The longline
299 model, which modeled catch with a single Poisson GAM, explained 67% of the deviance, yet
300 only had a Pearson correlation coefficient of 0.29.

301 The GAM response curves (Figure 4) for the trawl models generally showed similar
302 responses among concurrent variables between each P/A model and each CPUE model, relative
303 to the length of the timeseries. The primary exception is sediment size for the CPUE model,
304 which showed opposite impacts of larger (sediment >3mm) grain size. All GAMs showed a
305 negative relationship with BT, especially at temperatures greater than ~10°C. The longline model
306 showed a similar, albeit less-extreme pattern, but did not include temperatures greater than
307 12.2°C in the training data. The two short-timeseries models that had salinity available found
308 that likelihood of occurrence and projected abundance decrease as salinity rises, particularly over
309 34. Depth, despite its overall importance in every model, had different impacts on the P/A,
310 abundance, and longline predictions. Short P/A response was very positively influence by depth,
311 while the long series plateaued after a depth of ~50m. Longline depth was negatively influential,
312 and CPUE models were mostly neutral. The other three benthic habitat characteristics were not
313 significant in every model. Negative rugosity was detrimental in both P/A models. Four models
314 utilized BPI, although the effects are conflicting. Both P/A models included VRM, which had a
315 strong negative effect on skate likelihood. The longline model showed opposite effects of depth,
316 BPI, and sediment compared to the trawl models. Standard error of the predicted curves
317 increased in less common habitats (Figure 4).

Bottom Trawl Predictions

Both trawl models projected either decreases or no change in probability of occurrence by the 2055 period regardless of season or climate scenario (Figure 5). Deep basins in the central GOM were the most likely to have decreased probability of occurrence (30-50% decrease under RCP 8.5), while plateaus and coastal areas in the western GOM had less change (0-20% decrease). There was a seasonal shift with skate experiencing less of a decline in likelihood along the northern shore of the GOM in the spring, and a more severe (40-70%) decrease in the fall. RCP 4.5 followed similar geographic patterns, but projected decreases at a smaller degree of magnitude (Figure A2). The shallower coastal areas projected a 0-20% decreased likelihood, while the basins projected a decrease up to 40%. The short timeseries model projected fewer decreases than the long timeseries model (Figures 5, A2). Both 2055 periods and the 2100 RCP 4.5 period project similar spatial patterns and magnitude of decrease. The decrease in thorny skate likelihood becomes more pronounced by 2100 (Figures 6, A3). The plateaus in the western GOM in the spring and Northeast Channel in the fall project a relatively small decrease in likelihood (<30%), while the rest of the GOM projects 50-70% declines in likelihood. Likelihood of occurrence is already small throughout GB, but is projected to decline even more by 2100 (>70%).

These geographic patterns held when the P/A model was combined with the zero-truncated CPUE model (Figure 7). Under RCP 4.5, decreases in thorny skate abundance were projected in the GOM in both spring and fall in both trawl timeseries models. Using the long timeseries, skate abundance is projected to decrease 32% and 33% in the spring and fall, respectively. The short timeseries model projected decreases of 23% and 32% (Figure A4). The west side of the GOM was less impacted, projecting decreases of 0-20% in both long and short timeseries models, while the east was up to 50%. The southwest corner of the GOM projects the smallest decline in the short timeseries (0-10%). By 2100, all RCP 8.5 models projected large decreases throughout the GOM, with 72% in the long timeseries. The short timeseries, which showed fewer decreases (10-30%) in the coastal regions of the western GOM, just like the P/A models totaling a 60% decrease in the spring. By fall, the short series projected a decrease of 81% (Figure 8).

The long and short trawl series models project different mean abundances through the northeast US at all timeframes of the analysis. The short timeseries model showed a larger seasonal variation than the long series as well, especially in the less severe climate and time scenarios. However, despite the differing input data, they projected similar percentage decreases overall for both RCP scenarios and time periods (Figure 9).

Longline Predictions

While overall results were similar in both trawl models, the same was not true when comparing the trawl models to the longline model. Projections were only made for the spatial extent of the longline survey, so not all locations can be compared, however the longline model projected decreases up to 50% at the western shallow extent and increases up to 40% in the eastern area surrounding the plateaus. Despite these increases, overall abundance was still projected to decrease overall. By the 2055 period, skate are projected to decrease 44% in the spring regardless of RCP scenario and 10% and 20% in the fall under RCP 4.5 and RCP 8.5 (Figure 7). Decreases continue by 2100, reaching 65% by the fall (Figure 8).

## Discussion

We used five different GAMs and two observational datasets to determine how thorny skate off the northeastern US may be impacted by climate change. Models trained using the bottom trawl survey projected large decreases in thorny skate in the 2055 period and by the end of the century (Figure 9). Given the inertia of the climate system and how long it takes carbon to be naturally removed from the atmosphere, climate effects for the 2055 period are similar regardless of climate scenario. However, mitigation will have a large effect by the 2100 period. Reducing emissions to achieve the RCP 4.5 scenario will decrease the projected impacts on thorny skate abundance compared to RCP 8.5 by ~35% (Figures 8,9, A2-A5). This lagged effect is not unique to thorny skate, but does provide another example of how present mitigation efforts will have a long-term impact, even though some continued warming is inevitable due to emissions that have already occurred.

These projected decreases by the end of the century quantitatively support the NMFS fisheries climate vulnerability assessment, which elicited expert evaluation to determine that

thorny skate has both high chances of exposure to climate impacts and high sensitivity to those impacts, leading to a designation that the species were highly vulnerable to climate change (Hare et al. 2016). In a separate NMFS study, thorny skate were projected to lose ~25% of their habitat area under a $CO_2$ doubling scenario (Kleisner et al. 2017), estimating a similar change as a Canadian study modelling habitat with a 3°C SST increase (Shackell et al. 2014). In the latter study (Shackell et al. 2014), neither their metric nor their climate scenario is directly comparable to our abundance projections here, but our results would indicate that is a reasonable estimate. In our model and these other studies, increased water temperature is the driving force behind a continued decline in thorny skate abundance, particularly in the P/A models.

Thorny skate populations on the Scotian Shelf and Grand Banks have hyper-aggregated and maintained a low but stable abundance over the last several decades (Kulka et al. 2004; Simpson, Miri, and Collins 2016). However, migration to these historically suitable habitats is unlikely because these regions are warming rapidly for the same reasons as the GOM and thorny skate do not tend to move very far on their own accord (Templeman 1984; Kneebone et al. 2020). If thorny skate cannot easily move from the GOM or GB, our climate projections are even more concerning. We did not explicitly model movement or aggregation, but this could be useful for future thorny skate conservation concerns.

Despite the differing spatio-temporal coverage, available variables, and scale of CPUE between the long and the short trawl timeseries models, they both projected similar proportions of thorny skate decreases across the shelf as a whole. They also modelled the relationships between the response and predictor variables similarly. The lone exception was sediment size in the CPUE model of the long timeseries (Figure 4). Since the model is correlative, the variables may not necessarily be included or modelled in the same way. The overall similarity in model results of the two timeseries lengths is a useful finding for the efficiency of future studies that want to utilize the full length of the trawl survey. The coarse resolution of climate models is also unlikely to heavily impact results for this species. A supplemental investigation determined that, similar to a previous study (Grieve et al. 2017), a statistically downscaled GCM ensemble performed similarly to a 0.1° climate projection GFDL CM2.6, indicating that the lower resolution GCMs are functional for this type of study (Figure A6).

The longline survey has very limited spatio-temporal coverage compared to the bottom trawl survey, however the longline model is still useful to help consider the effects of the biases of the trawl survey and the low catchability of the thorny skate (Runnebaum et al. 2017). Despite the limited spatio-temporal coverage, the sampled thermal range of survey is unlikely to play a role in the longline results. Trends from the bottom trawl survey models were similar when they were trained with samples taken in the same thermal range as the longline (not shown). This indicates other features of the longline survey, such as the ability to sample structured habitat, were the primary drivers of the differences between the models. However, there may have been other effects of the longline sampling methodology unaccounted for. For example, spiny dogfish are more common in the fall, potentially saturating longline hooks and leading spring and fall catch disparity being opposite of the trawl surveys. Work is ongoing at NEFSC to include probabilistic hook saturation as an index for more detailed skate models, as has been conducted previously for Atlantic halibut (*Hippoglossus hippoglossus;* Smith 2016). Another factor could be the length of the longline placed over an area of different depths or where ETOPO was not an adequate representation of where the skate were fished at. Since all longline catches were presented as the middle of the longline, the high resolution of the added benthic variables may have led to a misrepresentation of the actual habitat the fish was occupying. This necessary spatial generalization may have had an impact on the initial model, but not on the 0.1° resolution of the predictions. Downscaling climate variables to the same resolution as the highest resolution benthic variable (0.003° BPI) was not computationally feasible.

Reconciling the longline and trawl surveys is difficult. The limited spatial area of the survey does not allow us to compare regions throughout the GOM and northeast US. In overlapping areas, the longline model shows increases in deeper waters. Decreases are still expected as climate continues to warm (Figure 8), but still projects at a lower rate. The projections from the longline model are less homogenous than the bottom trawl models, potentially a result of the survey methodology. The longline survey specifically targets complex habitats, leading to higher skate catches (Sosebee et al. 2016; McElroy et al. 2019). Bottom trawls, on the other hand, work best on relatively smooth, noncomplex habitats. Runnebaum et al (2017) developed a model standardizing catch between longline and trawl surveys for the data-limited demersal fish, cusk (*Brosme brosme*). They did this by standardizing area swept in each survey, modelling cusk density for each method, and using that modelled density as an input for

calculating a habitat suitability index. The resulting habitat suitability indices improved on modelling each method separately, albeit with high uncertainty due to multiplication of errors, simplification of survey details, and necessary assumptions (Runnebaum et al. 2017). This approach may supply a roadmap for the next steps in better quantifying how thorny skate will be affected by climate change, however combining this approach with climate models amplifies uncertainty even further (Hawkins and Sutton 2009).

There are several caveats to consider with this paper. We assumed that the distribution of thorny skate is driven by environmental factors including habitat, temperature, and salinity, but laboratory experiments or mechanistic models are necessary to verify this causal relationship (Jarnevich et al. 2015). Further, we did not account for non-environmental drivers such as species interactions, dispersal limitation, and historical fishing pressure, which could have influenced thorny skate population dynamics during the study period. Historical fishing pressure has drastically reduced the overall abundance of the species, and the realized habitat area is smaller than it would have been without that pressure. Abundance models attempt to differentiate between potential and realized habitats, but there is still variation as to what may actually occur (Wiens et al. 2009). Community interactions and species adaptation are not considered. It is unlikely that, given the slow reproduction times of the thorny skate, they could evolve quickly enough to make a substantial difference despite high genetic diversity and varying sizes of maturity (Sosebee 2005; Sulikowski et al. 2006; Lynghammar et al. 2014; NMFS 2017). Longline projections should be interpreted cautiously due to limited spatiotemporal data that trained the model.

The purpose of this study was twofold. First, to better estimate the impacts of climate change on thorny skate for an ESA petition and to expand these projections to 2100. To that end, thorny skate abundance is projected to continue to decrease 30-40% by mid-century and continue to ~70% by the end of the century if greenhouse gas emissions are not reduced to RCP4.5 levels. Second, we wished to investigate the effects of different sampling techniques on species abundance projections. Given the disparities between the bottom trawl and longline models, we encourage the continuation of both bottom trawl and longline surveys with spatio-temporal coverage along the entire Northeast US continental shelf. Future modeling efforts for other

465 demersal species in complex habitats may want to consider different survey methodologies if the
466 bottom trawl is inefficient at capturing the target species.

467 **Author Contributions**

468 BG and JH developed the methodology, BG conducted the analysis and wrote and
469 revised the manuscript, DM provided survey and species expertise, BG JH and DM edited the
470 manuscript.

471

472 **Figures**

473 Table 1: Variables included in each model. Asterisks denote significance level. Gray regions
474 indicate variables that were unavailable for the model, while dashes indicate the variable was
475 not included in the model with the lowest AIC. P-values are approximate and were not used for
476 model selection, but can show to what variables were included and their level of significance.

| | Source | Average spatial resolution | Short P/A | Short CPUE | Long P/A | Long CPUE | Longline CPUE |
|---|---|---|---|---|---|---|---|
| Bottom Temperature | NOAA World Ocean Atlas | 0.100° x 0.100° | ** | ** | *** | *** | *** |
| Bottom Salinity | NOAA World Ocean Atlas | 0.100° x 0.100° | *** | * | | | |
| Depth | ETOPO2 | 0.033° x 0.033° | *** | ** | *** | *** | *** |
| BPI | NAMERA | 0.003° x 0.003° | — | ** | *** | *** | *** |
| VRM | NAMERA | 0.003° x 0.003° | | — | * | — | *** |
| Rugosity | NAMERA | 0.004° x 0.004° | ** | * | *** | — | *** |
| Soft Sediment | NAMERA | 0.004° x 0.004° | *** | * | *** | *** | *** |
| Season | — | — | *** | *** | *** | *** | |
| Deviance Explained | | | 52.6 | 22 | 55.9 | 13.9 | 67.2 |
| Correlation | | | | 0.564 | | 0.645 | 0.287 |
| N† | | | 2465 | 428 | 7080 | 1556 | 123 |

| | | | | | |
|---|---|---|---|---|---|
| AUC‡ | | 0.948 | | 0.939 | |
| | * p<0.10 | ** p<0.01 | ***p<0.001 | | |
| † Number of samples<br>‡ Area under the curve | | | | | |

Table 2: Climate models included in the ensemble

| Climate Model | Average Spatial Resolution |
|---|---|
| CCCma-CanESM2 | 0.90° x 1.40° |
| CMCC-CMS | 1.20° x 2.0° |
| LASG-FGOALS-g2 | 0.90° x 1.0° |
| JAMSTEC-MIROC5 | 0.80° x 1.0° |
| MPI-ESM-MR | 0.50° x 0.50° |

**Figure Legends**

Figure 1: Mean thorny skate catch-per-unit-effort during two seasons and time periods from the NOAA Bottom Trawl Surveys. The Scotian Shelf has not been sampled by NOAA since 1986 and is not represented in the short timeseries. The 'Fall, long' subplot has some areas labeled that are referenced throughout the manuscript

Figure 2: (A,C) Projected changes in bottom temperature by the 2046-2065 period from the 1986-2005 period. (B,D) Standard deviation of projected temperature change in five different climate models.

Figure 3: (A,C) Projected changes in bottom temperature by the 2081-2100 period from the 1986-2005 period. (B,D) Standard deviation of projected temperature change in five different climate models.

Figure 4: Generalized additive model response curves for all models and variables. Curves represent the relative impact of each variable on the response. Shaded regions represent two standard error. Gray squares indicate variables either not included in the model (bottom salinity) or removed during selection (Rugosity, VRM). BT and BS indicate bottom temperature and salinity, rugosity, BPI, and VRM are measures of benthic complexity. See text for details.

Figure 5: Projected change in likelihood of thorny skate being present in an area by the 2046-2065 period from the 1986-2005 period under RCP 8.5. Subplots are split by season and length of training series.

Figure 6: Projected change in likelihood of thorny skate being present in an area by the 2081-2100 period from the 1986-2005 period under RCP 8.5. Subplots are split by season and length of training series.

Figure 7: Projected change in catch-per-unit-effort of thorny skate in an area by the 2046-2065 period from the 1986-2005 period under RCP 8.5. Subplots are split by season and capture methodology of training dataset. Bottom trawl models (A,B,D,E), are split by length of the training series

Figure 8: Projected change in catch-per-unit-effort of thorny skate in an area by the 2081-2100 period from the 1986-2005 period under RCP 8.5. Subplots are split by season and capture methodology of training dataset. Bottom trawl models (A,B,D,E), are split by length of the training series

Figure 9: Projected mean catch-per-unit-effort of thorny skate in the Gulf Of Maine. Individual climate model runs are indicated by thin colored lines while the ensemble average is bolded. Note the change in scale on the Y-axis.

**References**

Akaike, H. (1974). A new look at the statistical model identification. *IEEE Transactions on Automatic Control*, *19*(6), 716–723.

Azarovitz, T. (1981). A Brief Historical Review of the Woods Hole Laboratory Trawl Survey Time Series. *Bottom Trawl Surveys*.

Azarovitz, T., Clark, S., Despres, L., & Byrne, C. (1997). THE NORTHEAST FISHERIES SCIENCE CENTER BOTTOM TRAWL SURVEY PROGRAM. *ICES CM*.

Bell, R. J., Richardson, D. E., Hare, J. A., Lynch, P. D., & Fratantoni, P. S. (2015). Disentangling the effects of climate, abundance, and size on the distribution of marine fish: An example based on four stocks from the Northeast US shelf. *ICES Journal of Marine Science*, *72*(5), 1311–1322. doi: 10.1093/icesjms/fsu217

Brillant, S. W., Vanderlaan, A. S., Rangeley, R. W., & Taggart, C. T. (2015). Quantitative estimates of the movement and distribution of North Atlantic right whales along the northeast coast of North America. *Endangered Species Research*, *27*(2), 141-154. doi: https://doi.org/10.3354/esr00651

Cheung, W. W. L., Lam, V. W. Y., Sarmiento, J. L., Kearney, K., Watson, R., Zeller, D., & Pauly, D. (2010). Large-scale redistribution of maximum fisheries catch potential in the global ocean under climate change: CLIMATE CHANGE IMPACTS ON CATCH POTENTIAL. *Global Change Biology*, *16*(1), 24–35. doi: 10.1111/j.1365-2486.2009.01995.x

Davies, T. D., & Jonsen, I. D. (2011). Identifying nonproportionality of fishery-independent survey data to estimate population trends and assess recovery potential for cusk (*Brosme brosme*). *Canadian Journal of Fisheries and Aquatic Sciences*, *68*(3), 413–425. doi: 10.1139/F10-165

Edwards, R. L. (1968). Fishery Resources of the North Atlantic area. In D. Gilbert (Ed.), *The Future of the Fishing Industry in the United States*: *Vol. IV* (pp. 52–60). University of Washington Publications in Fisheries.

Federal Register. (2015). *Endangered and Threatened Wildlife; 90-Day Finding on a Petition To List the Thorny Skate as Threatened or Endangered Under the Endangered Species Act* (No. 80 FR 65175).

Federal Register. (2017). *Endangered and Threatened Wildlife and Plants; Notice of 12-Month Finding on a Petition To List Thorny Skate as Threatened or Endangered Under the Endangered Species Act (ESA)* (No. 82(36)).

Friedland, K. D., & Hare, J. A. (2007). Long-term trends and regime shifts in sea surface temperature on the continental shelf of the northeast United States. *Continental Shelf Research*, *27*(18), 2313–2328. doi: 10.1016/j.csr.2007.06.001

Greene, J. K., Anderson, M. G., Odell, J., & Steinberg, N. (2010). *The Northwest Atlantic Marine Ecoregional Assessment: Species, Habitats and Ecosystems. Phase One.* The Nature Conservancy, Eastern U.S. Division, Boston, MA.

559 Grieve, B., Curchitser, E., & Rykaczewski, R. (2016). Range expansion of the invasive lionfish in the
560 Northwest Atlantic with climate change. *Marine Ecology Progress Series*, *546*, 225–237. doi:
561 10.3354/meps11638

562 Grieve, B. D., Hare, J. A., & Saba, V. S. (2017). Projecting the effects of climate change on Calanus
563 finmarchicus distribution within the U.S. Northeast Continental Shelf. *Scientific Reports*, *7*(1).
564 doi: 10.1038/s41598-017-06524-1

565 Guisan, A., Edwards, T. C., & Hastie, T. (2002). Generalized linear and generalized additive models in
566 studies of species distributions: Setting the scene. *Ecological Modelling*, *157*(2), 89–100.

567 Hare, J. A., Manderson, J. P., Nye, J. A., Alexander, M. A., Auster, P. J., Borggaard, D. L., … Biegel, S.
568 T. (2012). Cusk (Brosme brosme) and climate change: Assessing the threat to a candidate marine
569 fish species under the US Endangered Species Act. *ICES Journal of Marine Science*, *69*(10),
570 1753–1768. doi: 10.1093/icesjms/fss160

571 Hare, Jonathan A., Morrison, W. E., Nelson, M. W., Stachura, M. M., Teeters, E. J., Griffis, R. B., …
572 Griswold, C. A. (2016). A Vulnerability Assessment of Fish and Invertebrates to Climate Change
573 on the Northeast U.S. Continental Shelf. *PLOS ONE*, *11*(2), e0146756. doi:
574 10.1371/journal.pone.0146756

575 Hawkins, E., & Sutton, R. (2009). The Potential to Narrow Uncertainty in Regional Climate Predictions.
576 *Bulletin of the American Meteorological Society*, *90*(8), 1095–1108. doi:
577 10.1175/2009BAMS2607.1

578 Hoegh-Guldberg, O., & Bruno, J. F. (2010). The impact of climate change on the world's marine
579 ecosystems. *Science*, *328*, 1523–1528.

580 IPCC. (2013). *Summary for Policy Makers. In: Climate Change 2013: The Physical Science Basis.*
581 *Contribution of Working Group I to the Fifth Assessment Report of the Intergovernmental Panel*
582 *on Climate Change*. Cambridge, United Kingdom and New York, NY, USA: Cambridge
583 University Press.

584 Jarnevich, C. S., Stohlgren, T. J., Kumar, S., Morisette, J. T., & Holcombe, T. R. (2015). Caveats for
585 correlative species distribution modeling. *Ecological Informatics*, *29*, 6–15. doi:
586 10.1016/j.ecoinf.2015.06.007

Kleisner, K. M., Fogarty, M. J., McGee, S., Hare, J. A., Moret, S., Perretti, C. T., & Saba, V. S. (2017). Marine species distribution shifts on the U.S. Northeast Continental Shelf under continued ocean warming. *Progress in Oceanography*, *153*, 24–36. doi: 10.1016/j.pocean.2017.04.001

Kneebone, J., Sulikowski, J., Knotek, R., McElroy, W. D., Gervelis, B., Curtis, T., … Mandelman, J. (2020). Using conventional and pop-up satellite transmitting tags to assess the horizontal movements and habitat use of thorny skate (*Amblyraja radiata*) in the Gulf of Maine. *ICES Journal of Marine Science, in press.* doi: *10.1093/icesjms/fsaa149*

Kulka, D. W., Miri, C. M., Simpson, M. R., & Sosebee, K. A. (2004). Thorny skate (*Amblyraja radiata* Donovan, 1808) on the Grand Banks of Newfoundland. *Northwest Atlantic Fisheries Organization*, *SCR Doc 04/35*.

Lo, N. C., Jacobson, L. D., & Squire, J. L. (1992). Indices of Relative Abundance from Fish Spotter Data based on Delta-Lognormal Models. *Canadian Journal of Fisheries and Aquatic Sciences*, *49*, 2515–2526.

Locarnini, R. A., Mishonov, A. V., Antonov, J. I., Boyer, T. P., Garcia, H. E., Baranova, O. K., … Seidov, D. (2013). *World Ocean Atlas 2013, Volume 1: Temperature*.

Lundblad, E. R., Wright, D. J., Miller, J., Larkin, E. M., Rinehart, R., Naar, D. F., … Battista, T. (2006). A Benthic Terrain Classification Scheme for American Samoa. *Marine Geodesy*, *29*(2), 89–111. doi: 10.1080/01490410600738021

Lynghammar, A., Christiansen, J. S., Griffiths, A. M., Fevolden, S.-E., Hop, H., & Bakken, T. (2014). DNA barcoding of the northern Northeast Atlantic skates (*Chondrichthyes, Rajiformes*), with remarks on the widely distributed starry ray. *Zoologica Scripta*, *43*, 485–495.

Mathworks Inc. (2019). MATLAB and Statistics Toolbox Release 2019b (Version 2019b). Natick, Massachusetts, United States: Mathworks Inc.

McEachran, J. D., & Musick, J. A. (1975). DISTRIBUTION AND RELATIVE ABUNDANCE OF SEVEN SPECIES OF SKATES (PISCES: RAJIDAE) WHICH OCCUR BETWEEN NOVA SCOTIA AND CAPE HATTERASl. *FISHERY BULLETIN*, *73*, 27.

McElroy, D., O'Brien, L., Blaylock, J., Martin, M., H., Rago, P. J., Hoey, J. J., & Sheremet, V. A. (2019). Design, Implementation, and Results of a Cooperative Research Gulf of Maine Longline Survey, 2014-2017. *NOAA Technical Memorandum*, *NMFS-NE-249*, 161.

McMullen, K. Y., Paskevich, V. F., & Poppe, L. J. (2014). GIS data catalog (ver. 3.0, November 2014). In L. J. Poppe, K. Y. McMullen, S. J. Williams, & V. F. Paskevich (Eds.), *USGS east-coast sediment analysis: Procedures, database, and GIS data*. U.S. Geological Survey Open-File Report 2005-1001.

Morley, J. W., Selden, R. L., Latour, R. J., Frölicher, T. L., Seagraves, R. J., & Pinsky, M. L. (2018). Projecting shifts in thermal habitat for 686 species on the North American continental shelf. *PLOS ONE*, *13*(5), e0196127. doi: 10.1371/journal.pone.0196127

Moss, R. H., Edmonds, J. A., Hibbard, K. A., Manning, M. R., Rose, S. K., van Vuuren, D. P., … Wilbanks, T. J. (2010). The next generation of scenarios for climate change research and assessment. *Nature*, *463*(7282), 747–756. doi: 10.1038/nature08823

National Geophysical Data Center. (2006). *2-minute Gridded Global Relief Data (ETOPO2) v2*. National Geophysical Data Center, NOAA.

New England Fishery Management Council. (2003). *Northeast Skate Complex Management Plan*.

NMFS. (2017). *Status review report: Thorny Skate (*Amblyraja radiata*). Final Report to National Marine Fisheries Service, Office of Protected Resources* (No. Status Review Report).

NMFS. (2018). *Fisheries of the Northeastern United States; Northeast Skate Complex; Framework Adjustment 5 and 2018-2019 Specifications* (Rule No. 83 FR 48985; pp. 48985–48989). National Oceanic and Atmospheric Administration.

Nye, J., Link, J., Hare, J., & Overholtz, W. (2009). Changing spatial distribution of fish stocks in relation to climate and population size on the Northeast United States continental shelf. *Marine Ecology Progress Series*, *393*, 111–129. doi: 10.3354/meps08220

Packer, D. B., Zetlin, C. A., & Vitaliano, J. J. (2003). Thorny Skate, *Amblyraja radiata*, life history and habitat characteristics. *NOAA Technical Memorandum*, *NMFS-NE-178*.

Parmesan, C., & Yohe, G. (2003). A globally coherent fingerprint of climate change impacts across natural systems. *Nature*, *421*, 37–42. doi: 10.1038/nature01286

641 Perry, A. L. (2005). Climate Change and Distribution Shifts in Marine Fishes. *Science*, *308*(5730), 1912–
642 1915. doi: 10.1126/science.1111322

643 Pershing, A. J., Alexander, M. A., Hernandez, C. M., Kerr, L. A., Le Bris, A., Mills, K. E., … Thomas, A.
644 C. (2015). Slow adaptation in the face of rapid warming leads to collapse of the Gulf of Maine
645 cod fishery. *Science*, *350*(6262), 809–812.

646 Poloczanska, E. S., Brown, C. J., Sydeman, W. J., Kiessling, W., Schoeman, D. S., Moore, P. J., …
647 Richardson, A. J. (2013). Global imprint of climate change on marine life. *Nature Climate*
648 *Change*, *3*(10), 919–925. doi: 10.1038/nclimate1958

649 R Core Team. (2017). R: A language and environment for statistical computing. Retrieved from R
650 Foundation for Statistical Computing, Vienna, Austria website: https://www.R-project.org

651 Robin, X., Turck, N., Hainard, A., Tiberti, N., Lisacek, F., Sanchez, J.-C., & Müller, M. (2011). pROC:
652 An open-source package for R and S+ to analyze and compare ROC curves. *BMC Bioinformatics*,
653 *12*(1), 77.

654 Runnebaum, J., Guan, L., Cao, J., O'Brien, L., & Chen, Y. (2017). Habitat suitability modeling based on
655 a spatio-temporal model: An example for Cusk in the Gulf of Maine. *Canadian Journal of*
656 *Fisheries and Aquatic Sciences*. doi: 10.1139/cjfas-2017-0316

657 Sappington, J. M., Longshore, K. M., & Thompson, D. B. (2007). Quantifying Landscape Ruggedness for
658 Animal Habitat Analysis: A Case Study Using Bighorn Sheep in the Mojave Desert. *Journal of*
659 *Wildlife Management*, *71*(5), 1419–1426. doi: 10.2193/2005-723

660 Scott, W. B., & Scott, M. G. (1988). *Atlantic fishes of Canada*. Fisheries and Oceans Canada.

661 Shackell, N. L., Ricard, D., & Stortini, C. (2014). Thermal Habitat Index of Many Northwest Atlantic
662 Temperate Species Stays Neutral under Warming Projected for 2030 but Changes Radically by
663 2060. *PLoS ONE*, *9*(3), e90662. doi: 10.1371/journal.pone.0090662

664 Simpson, M. R., Miri, C. M., & Collins, R. K. (2016). Assessment of Thorny Skate (*Amblyraja radiata*
665 Donovan, 1808) in NAFO Divisions 3LNO and Subdivision 3Ps. *Northwest Atlantic Fisheries*
666 *Organization*, *SCR Doc 16/32*.

667 Smith, S. J. (2016). Review of the Atlantic halibut longline survey index of exploitable biomass.
668 *Canadian Technical Report of Fisheries and Aquatic Sciences*, *3180*. doi:
669 10.13140/rg.2.2.16025.21603

670 Sosebee, K.A. (2005). Maturity of Skates in Northeast United States Waters. *Journal of Northwest*
671 *Atlantic Fishery Science*, *35*, 141–153. doi: 10.2960/J.v35.m499

672 Sosebee, Katherine A., O'Brien Loretta, McElroy, D., & Sherman, S. (2016). *Update of thorny skate*
673 *(Amblyraja radiata) commercial and survey data* (p. ). doi: 10.7289/v5/rd-nefsc-16-08

674 Stock, C. A., Alexander, M. A., Bond, N. A., Brander, K. M., Cheung, W. W. L., Curchitser, E. N., …
675 Werner, F. E. (2011). On the use of IPCC-class models to assess the impact of climate on Living
676 Marine Resources. *Progress in Oceanography*, *88*(1–4), 1–27. doi: 10.1016/j.pocean.2010.09.001

677 Sulikowski, J. A., Kneebone, J., Elzey, S., Jurek, J., Howell, W. H., & Tsang, P. C. W. (2006). Using the
678 composite variables of reproductive morphology, histology and steroid hormones to determine
679 age and size at sexual maturity for the thorny skate *Amblyraja radiata* in the western Gulf of
680 Maine. *Journal of Fish Biology*, *69*(5), 1449–1465. doi: 10.1111/j.1095-8649.2006.01207.x

681 Templeman, W. (1984). Migrations of Thorny Skate, *Raja radiata* tagged in the Newfoundland Area.
682 *Journal of Northwest Atlantic Fishery Science*, *5*, 55–63. doi: 10.2960/J.v5.a12

683 Wiens, J. A., Stralberg, D., Jongsomjit, D., Howell, C. A., & Snyder, M. A. (2009). Niches, models, and
684 climate change: Assessing the assumptions and uncertainties. *Proceedings of the National*
685 *Academy of Sciences*, *106*(Supplement_2), 19729–19736. doi: 10.1073/pnas.0901639106

686 Wood, S. (2006). *Generalized additive models: An introduction with R*. CRC press.

687 Zweng, M. M., Reagan, J. R., Antonov, J. I., Locarnini, R. A., Mishonov, A. V., Boyer, T. P., … Biddle,
688 M. M. (2013). *World Ocean Atlas 2013, Volume 2: Salinity*.

689

**Appendix 1**

**Trawl survey methodology**

In 2009, the NOAA survey vessel R/V Albatross was retired and replaced with the FR/V H.B. Bigelow, which has a different capture efficiency for thorny skate (Brown et al. 2007; Miller et al. 2010). For years 2009-2012, catch from the Bigelow was converted to Albatross units using results from a calibration experiment (Miller et al. 2010). In both surveys, a stratified random design was used to select stations. In the Albatross era, a #36 or #41 Yankee bottom trawl was towed at 1.8 m/s for 30 minutes at each station, while the Bigelow towed a 4 seam, 3 bridle trawl at 1.5 m/s for 20 minutes (Reid, Almeida, and Zetlin 1999; Politis et al. 2014).

**Longline survey methodology**

The survey has a random stratified design based on the bottom trawl survey design and is further stratified by rough and smooth bottom type. In this survey, 1 nm lines containing 1000 #12 semi-circle easy-baiter hooks baited with squid were placed near the ocean bottom for two hours over the slack tide. Due to set and haul time, hooks at each end may have varied in soak time by up to 15 minutes

**Downscaled GFDL CM2.6 Comparison**

Due to the low abundance and catchability of thorny skate, it is important to use high-resolution climate projections. Climate models (GCMs) are coarse representations of the future climate (Stock et al. 2011). These can be statistically downscaled to higher resolutions, however important fine-scale oceanographic processes are still not resolved in projecting future temperatures (Saba et al. 2016), potentially having an impact on species projections. Grieve et al (Grieve, Hare, and Saba 2017) compared Calanus finmarchicus density with climate change using both a statistically downscaled GCM ensemble and a 0.10° high resolution ocean model and found that results were similar, but projected abundance using the high-resolution ocean model were greater likely due to the degree of warming in the Northeast Channel and shelf break due to the northern shift of the Gulf Stream (Grieve et al. 2017).

To examine how the coarse resolution of the climate models could impact our projections, an ensemble of downscaled GCMs and a single high-resolution GCM were used on all three datasets described above.

Despite statistically downscaling our ensemble of climate models, it is likely that fine scale oceanographic features behave differently when included in a climate model, as opposed to adding the coarse change to a climatology. We ran the same statistical models with both the downscaled ensemble and GFDL CM 2.6, which uses an 80-year Transient Climate Response scenario. This scenario adds 1% $CO_2$ per year, eventually doubling by year 70. This resulting sea surface temperature increase is roughly equivalent to the sea surface temperatures during the 2060's of RCP 8.5. Due to different forcings, it is not expected that this scenario would have equivalent projections to the downscaled ensemble but does provide a useful idea where the ensemble may be geographically biased.

We compared the projections from the downscaled climate model ensemble to the high-resolution GFDL CM2.6. The CM2.6 projections are similar to the ensemble-mean projections of both trawl series in both the present and future time periods of the matched TCS experiment (Pearson's correlation between 0.802 and 0.932 for each survey methodology and time frame). However, in all survey methodologies, the high-resolution model projected greater decreases in thorny skate abundance in GB, the Northeast Channel, and the eastern GOM (Figure A6). Overall, GFDL CM2.6 projected a 15-20% greater decrease in thorny skate abundance in the region than the ensemble, a trend driven by GB. Southern GB and the shelf break were areas poorly resolved by the coarse climate models. This is obvious in projections such as CanESM, where the coarse resolution was unable to account for rapidly changing oceanographic features (not shown). GFDL also projected a smaller decrease in the western GOM in the shallow banks north of Cape Cod (Figure A6).

Statistical downscaling with the delta approach used here is a useful way to preserve ocean features present in the climatology, but not the coarse climate models (Stock et al. 2011; Roberts 2017). However, these features may be reacting differently when included in the climate simulations, as opposed to remaining static. GFDL CM2.6 improves on this because it was run at a 25x higher resolution (0.1°) than the highest resolution climate model in the ensemble (MPI-ESM-MR; 0.5°). Despite that, each time period in GFDL CM2.6 had at least a 0.803 correlation with the roughly equivalent RCP ensemble time period. This is encouraging, indicating that the resolution of the BT component is not limiting the model, but there are important geographic distinctions. Primarily, the ensemble may underestimate a northern shift in the Gulf Stream

which results in warm, salty water entering the GOM (Saba et al. 2016). This same pattern was found to impact C. finmarchicus projections in the region as well (Grieve et al. 2017). Another study modelling thorny skate using GFDL CM2.6 also projected large decreases in thermal habitat area (Kleisner et al. 2017).



**References**

Brown, R. W., M. J. Fogarty, C. Legault, T. Miller, V. Nordahl, P. Politis, and P. Rago. 2007. "Survey Transition and Calibration of Bottom Trawl Surveys along the Northeastern Continental Shelf of the United States." ICEM CM2007/Q:20.

Grieve, Brian D., Jon A. Hare, and Vincent S. Saba. 2017. "Projecting the Effects of Climate Change on Calanus Finmarchicus Distribution within the U.S. Northeast Continental Shelf." Scientific Reports 7(1).

Kleisner, Kristin M., Michael J. Fogarty, Sally McGee, Jonathan A. Hare, Skye Moret, Charles T. Perretti, and Vincent S. Saba. 2017. "Marine Species Distribution Shifts on the U.S. Northeast Continental Shelf under Continued Ocean Warming." Progress in Oceanography 153:24–36.

Mathworks Inc. 2019. MATLAB and Statistics Toolbox Release 2019b. Natick, Massachusetts, United States: Mathworks Inc.

Miller, T. J., C. Das, P. J. Politis, A. S. Miller, S. M. Lucey, C. M. Legault, R. W. Brown, and P. J. Rago. 2010. "Estimation of Albatross IV to Henry B. Bigelow Calibration Factors." NEFSC Reference Document 10–05.

Politis, P. J., John K. Galbraith, Paul Kostovick, and Russell W. Brown. 2014. "Northeast Fisheries Science Center Bottom Trawl Survey Protocols for the NOAA Ship Henry B Bigelow." NEFSC Reference Document 14–06:138.

R Core Team. 2017. "R: A Language and Environment for Statistical Computing." R Foundation for Statistical Computing, Vienna, Austria. Retrieved (https://www.R-project.org).

Reid, Robert N., Frank P. Almeida, and Christine A. Zetlin. 1999. "Fishery-Independent Surveys, Data Sources, and Methods." NOAA Technical Memorandum NMFS-NE-122.

Roberts, Sarah. 2017. "Analzying the Spatial Distribution of Fish Species along the Mid and South Atlantic Bights and Projecting Future Distributions under a Climate Change Scenario." 44.

Robin, Xavier, Natacha Turck, Alexandre Hainard, Natalia Tiberti, Frédérique Lisacek, Jean-Charles Sanchez, and Markus Müller. 2011. "PROC: An Open-Source Package for R and S+ to Analyze and Compare ROC Curves." BMC Bioinformatics 12(1):77.

Saba, Vincent S., Stephen M. Griffies, Whit G. Anderson, Michael Winton, Michael A. Alexander, Thomas L. Delworth, Jonathan A. Hare, Matthew J. Harrison, Anthony Rosati, Gabriel A. Vecchi, and Rong Zhang. 2016. "Enhanced Warming of the Northwest Atlantic Ocean under Climate Change." Journal of Geophysical Research: Oceans 121(1):118–32.

Stock, Charles A., Michael A. Alexander, Nicholas A. Bond, Keith M. Brander, William W. L. Cheung, Enrique N. Curchitser, Thomas L. Delworth, John P. Dunne, Stephen M. Griffies, Melissa A. Haltuch, Jonathan A. Hare, Anne B. Hollowed, Patrick Lehodey, Simon A. Levin, Jason S. Link, Kenneth A. Rose, Ryan R. Rykaczewski, Jorge L. Sarmiento, Ronald J. Stouffer, Franklin B. Schwing, Gabriel A. Vecchi, and Francisco E. Werner. 2011. "On the Use of IPCC-Class Models to Assess the Impact of Climate on Living Marine Resources." Progress in Oceanography 88(1–4):1–27.

Wood, Simon. 2006. Generalized Additive Models: An Introduction with R. CRC press.

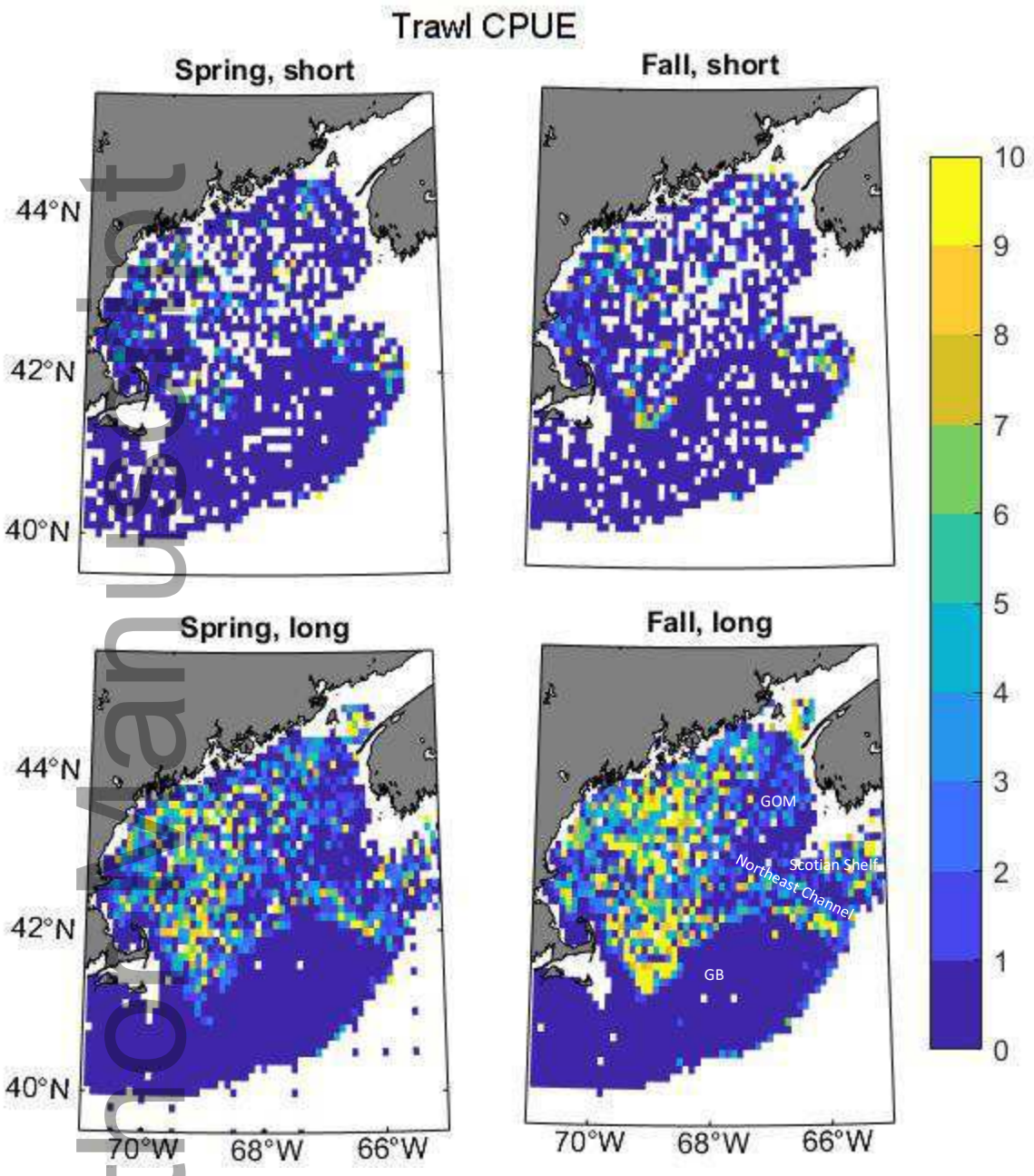


Figure 1: Mean thorny skate catch-per-unit-effort during two seasons and time periods from the NOAA Bottom Trawl Surveys. The Scotian Shelf has not been sampled by NOAA since 1986 and is not represented in the short timeseries. The 'Fall, long' subplot has some areas labeled that are referenced throughout the manuscript

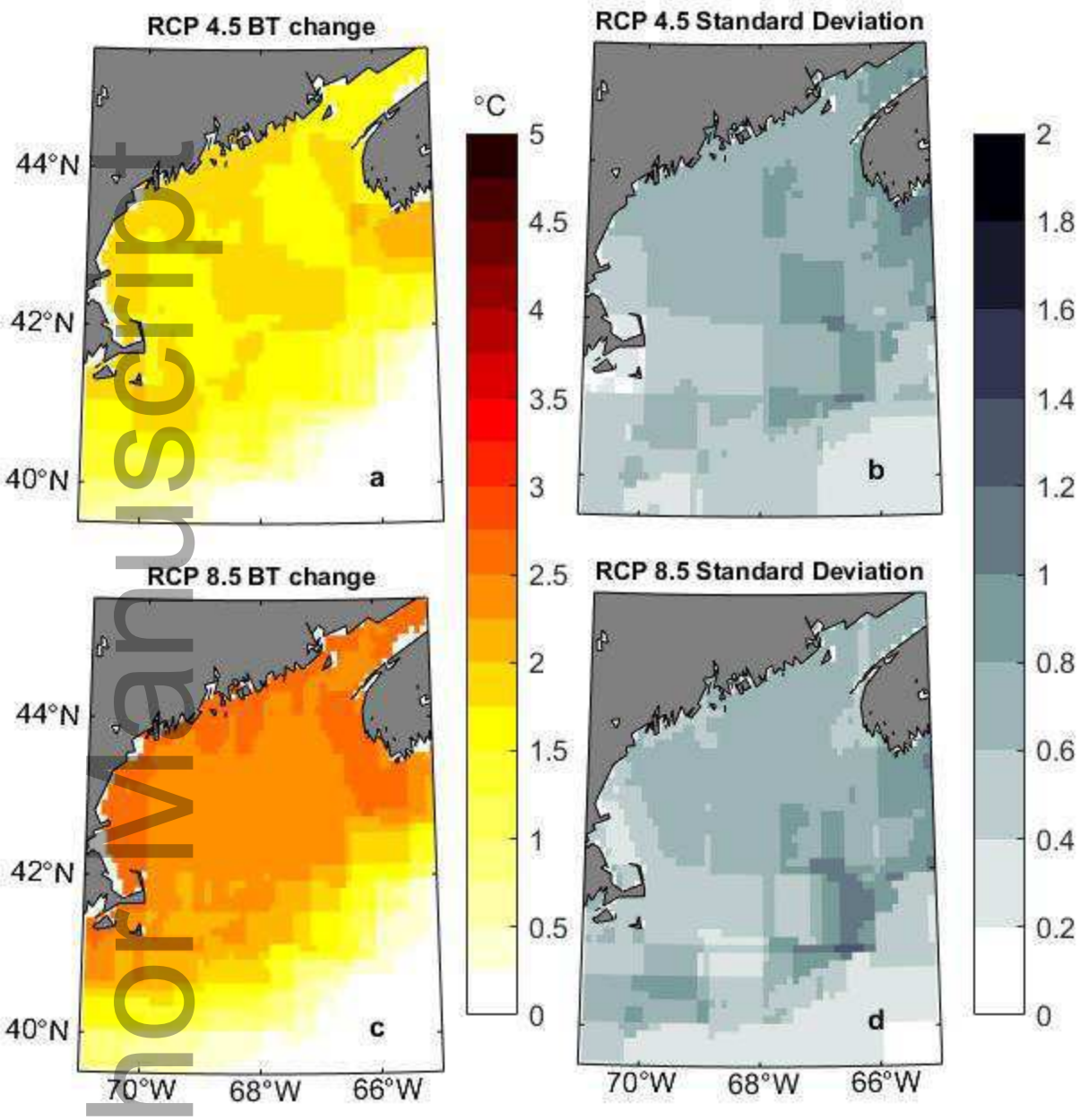


Figure 2: (A,C) Projected changes in bottom temperature by the 2046-2065 period from the 1986-2005 period. (B,D) Standard deviation of projected temperature change in five different climate models.

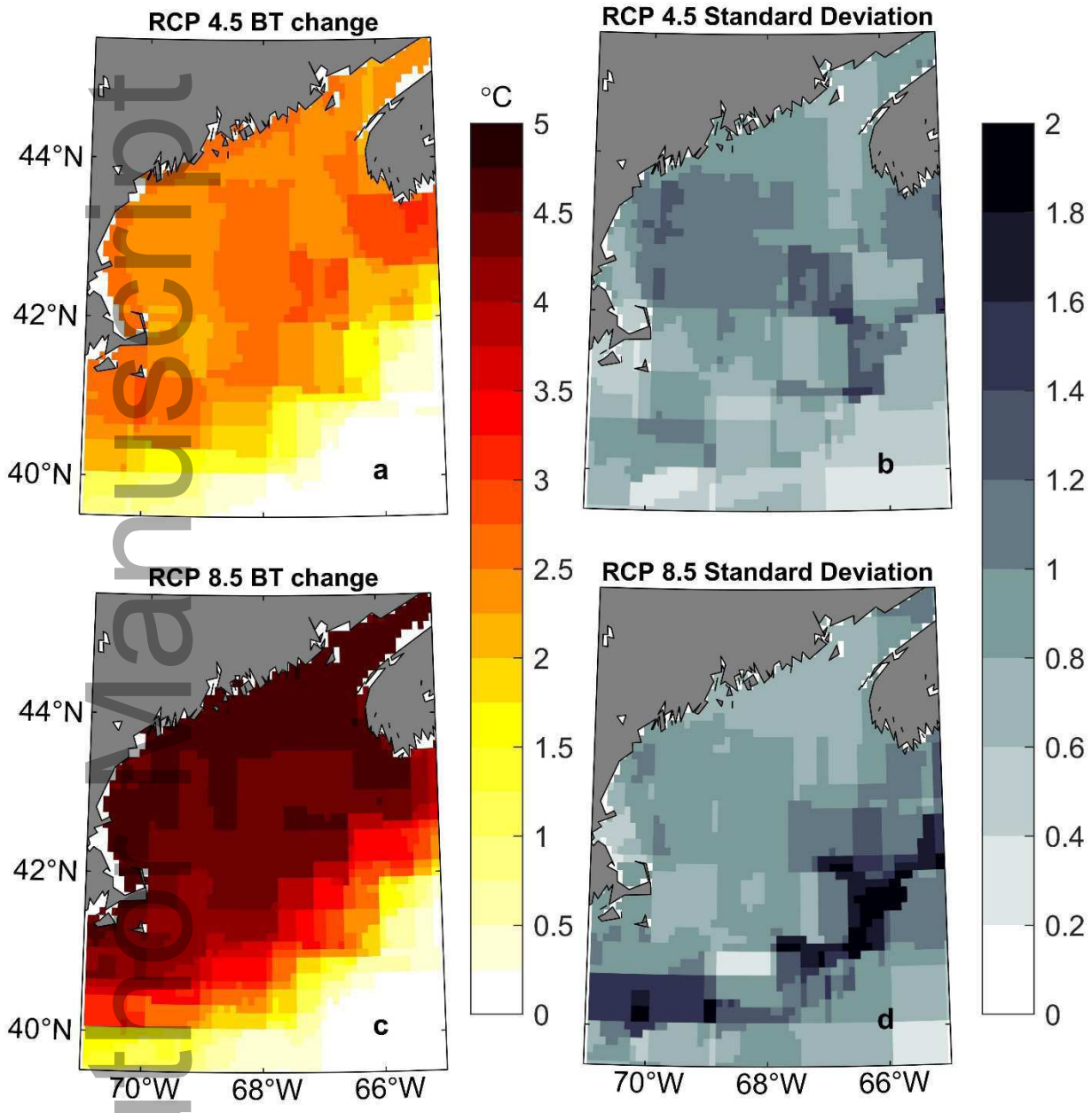


Figure 3: (A,C) Projected changes in bottom temperature by the 2081-2100 period from the 1986-2005 period. (B,D) Standard deviation of projected temperature change in five different climate models.

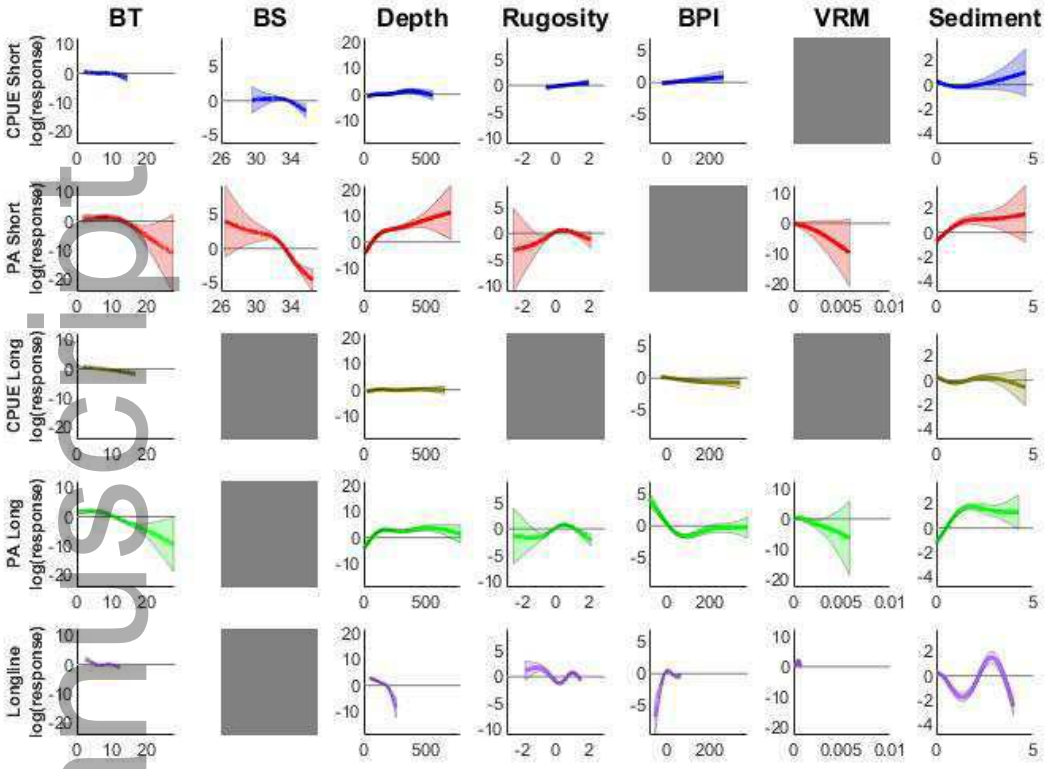


Figure 4: Generalized additive model response curves for all models and variables. Curves represent the relative impact of each variable on the response. Shaded regions represent two standard error. Gray squares indicate variables either not included in the model (bottom salinity) or removed during selection (Rugosity, VRM). BT and BS indicate bottom temperature and salinity, rugosity, BPI, and VRM are measures of benthic complexity. See text for details.

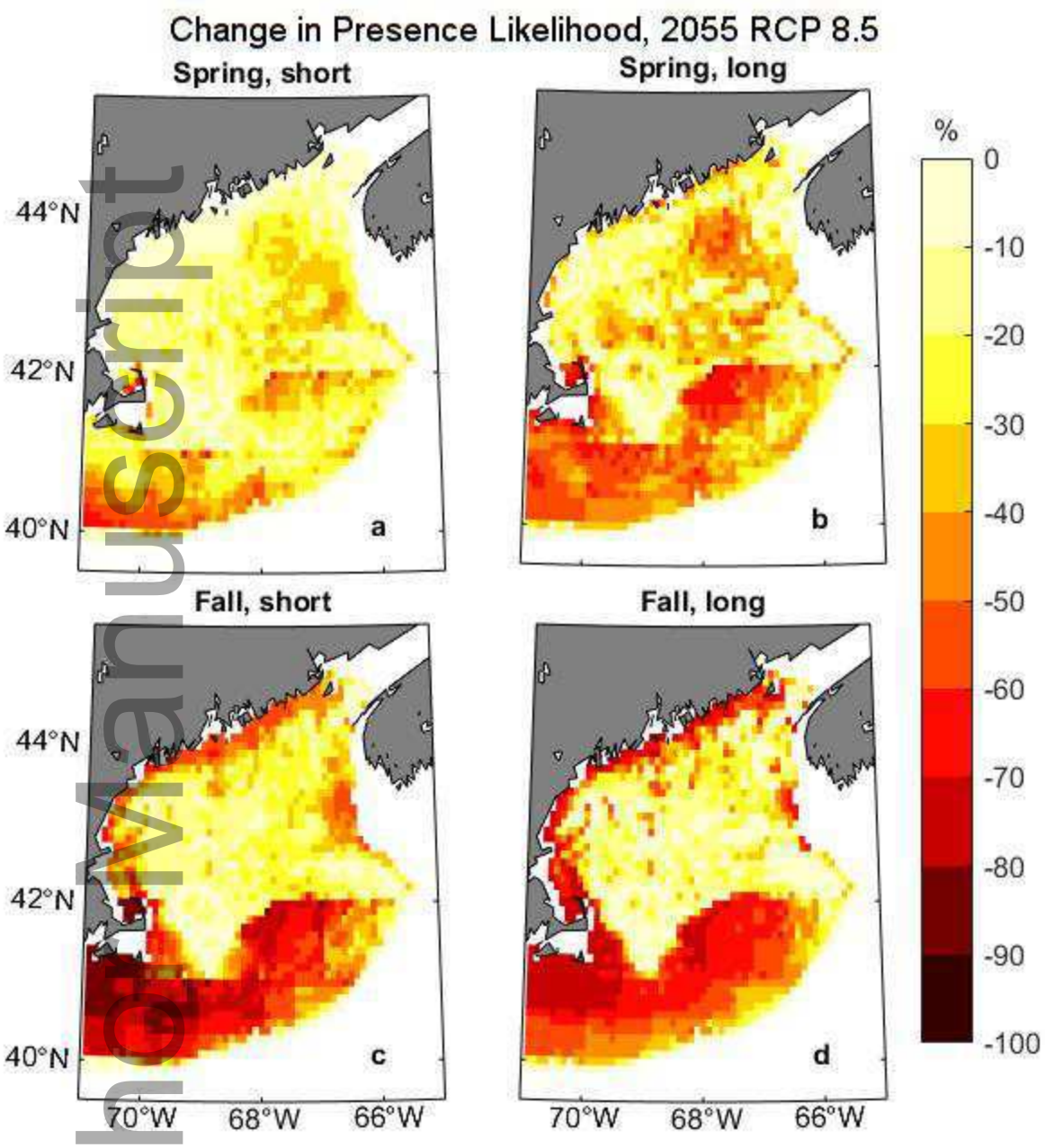


Figure 5: Projected change in likelihood of thorny skate being present in an area by the 2046-2065 period from the 1986-2005 period under RCP 8.5. Subplots are split by season and length of training series.

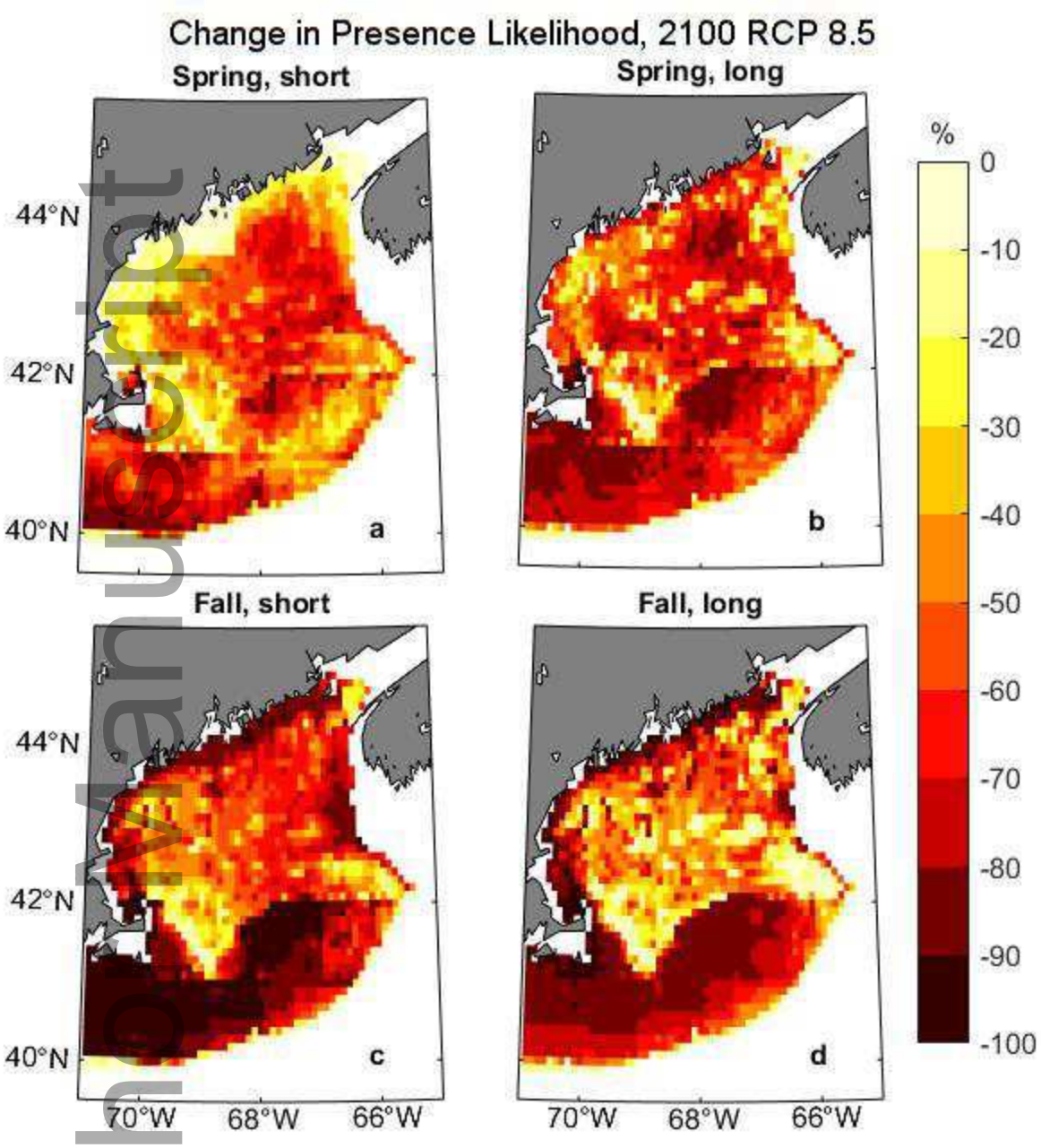


Figure 6: Projected change in likelihood of thorny skate being present in an area by the 2081-2100 period from the 1986-2005 period under RCP 8.5. Subplots are split by season and length of training series.

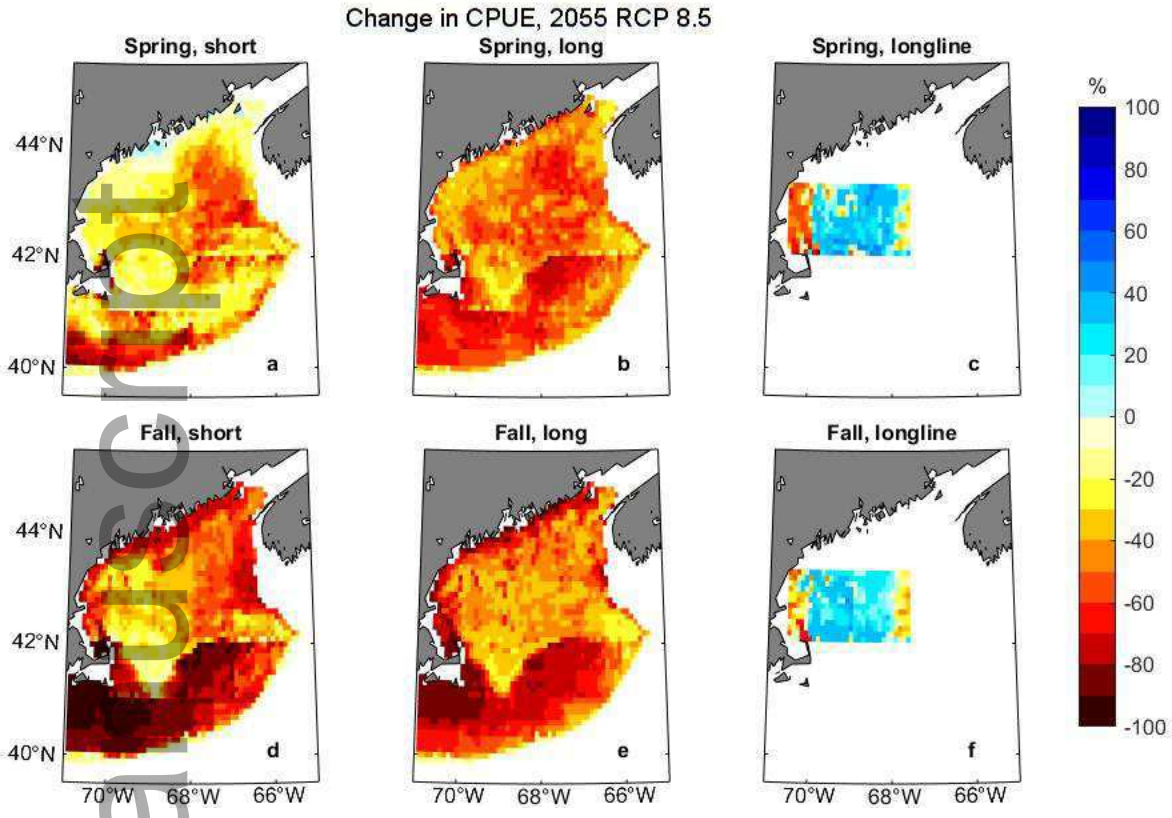


Figure 7: Projected change in catch-per-unit-effort of thorny skate in an area by the 2046-2065 period from the 1986-2005 period under RCP 8.5. Subplots are split by season and capture methodology of training dataset. Bottom trawl models (A,B,D,E), are split by length of the training series

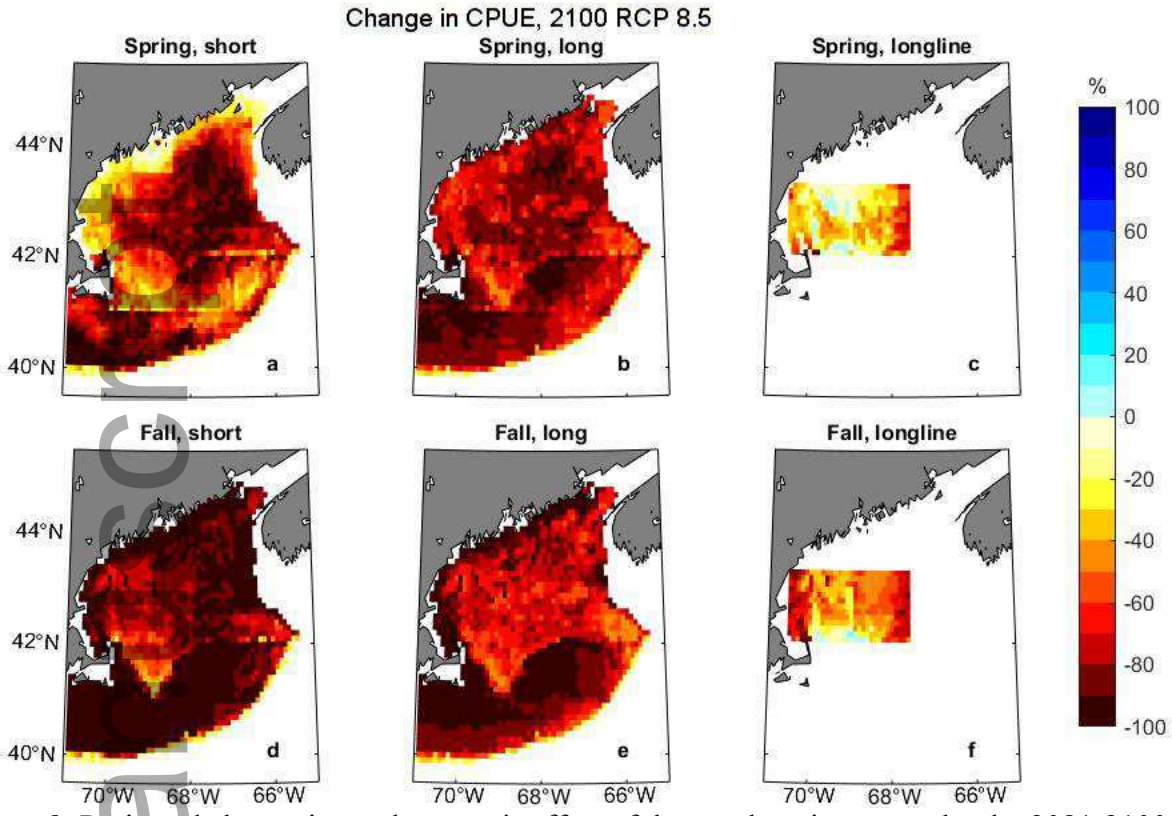


Figure 8: Projected change in catch-per-unit-effort of thorny skate in an area by the 2081-2100 period from the 1986-2005 period under RCP 8.5. Subplots are split by season and capture methodology of training dataset. Bottom trawl models (A,B,D,E), are split by length of the training series

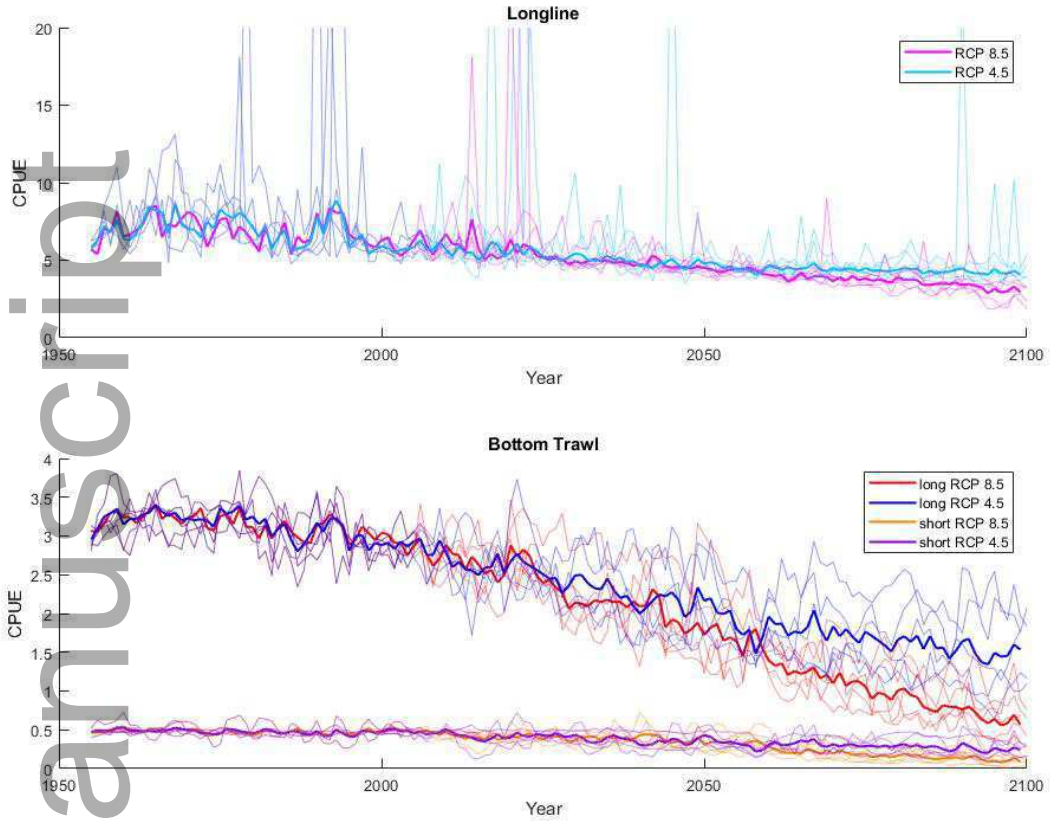


Figure 9: Projected mean catch-per-unit-effort of thorny skate in the Gulf of Maine and Georges Bank. Individual climate model runs are indicated by thin colored lines while the ensemble average is bolded. Note the change in scale on the Y-axis.

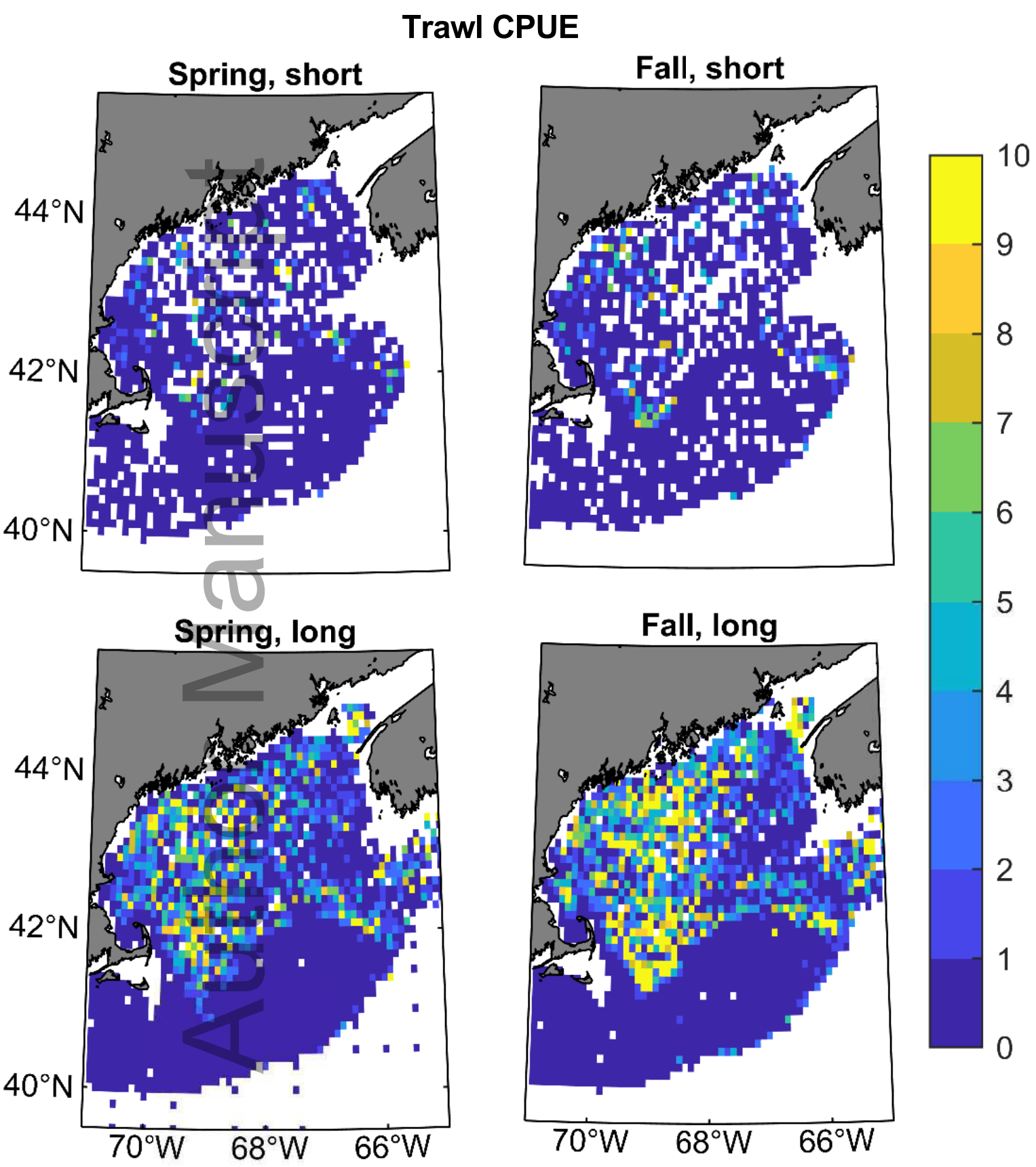


fog_12520_f1.eps

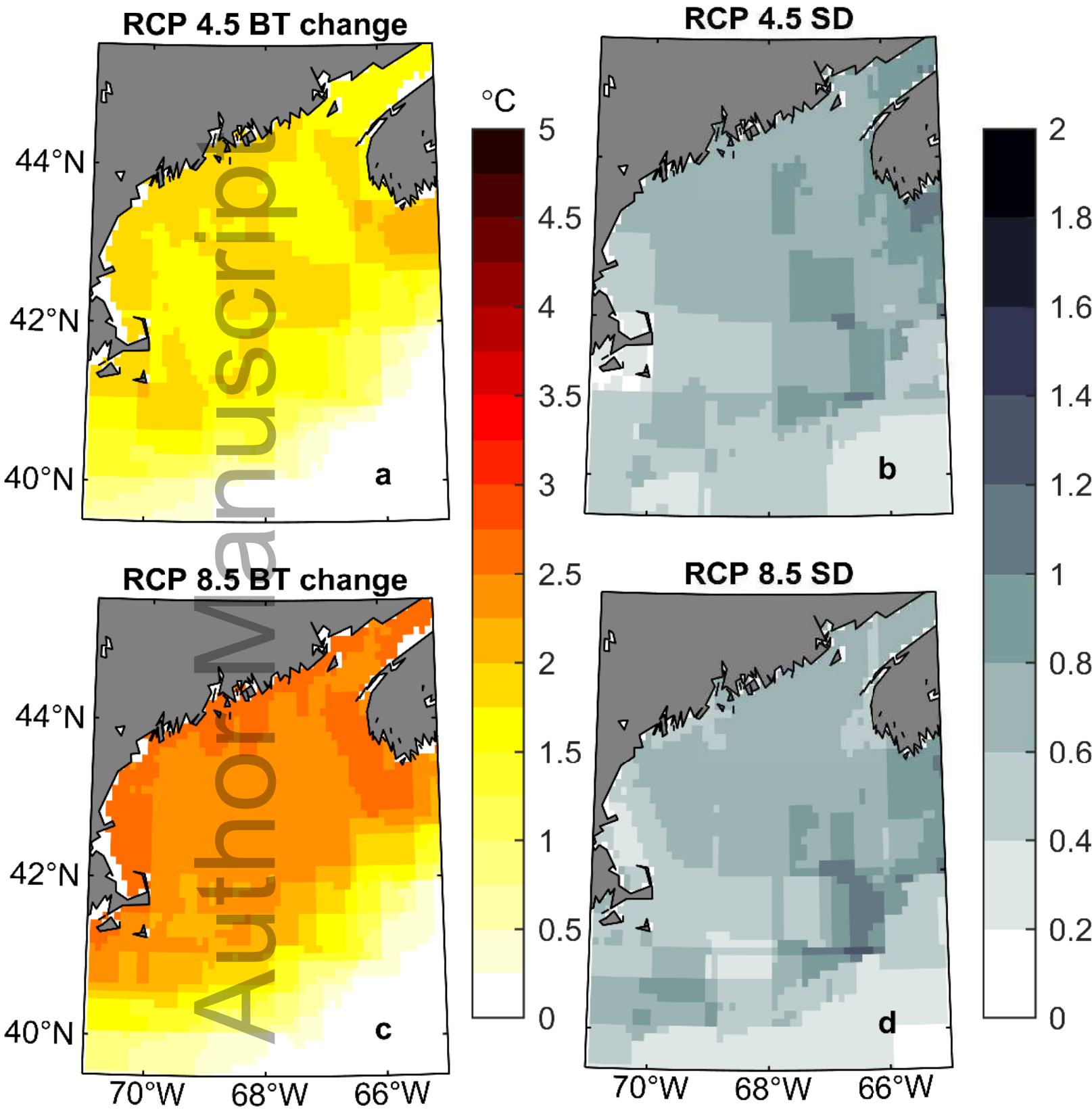




fog_12520_f2.eps

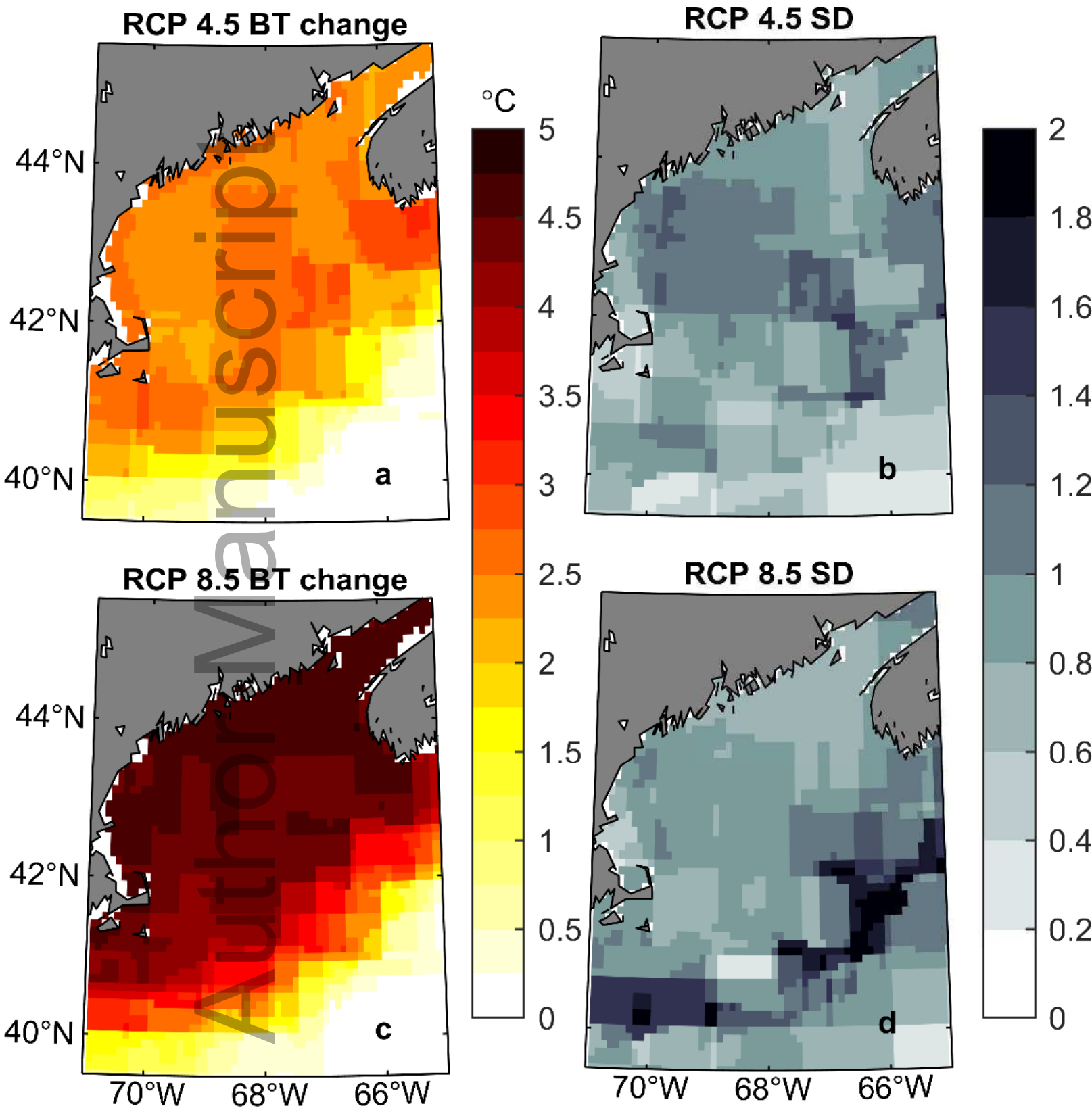




fog_12520_f3.eps

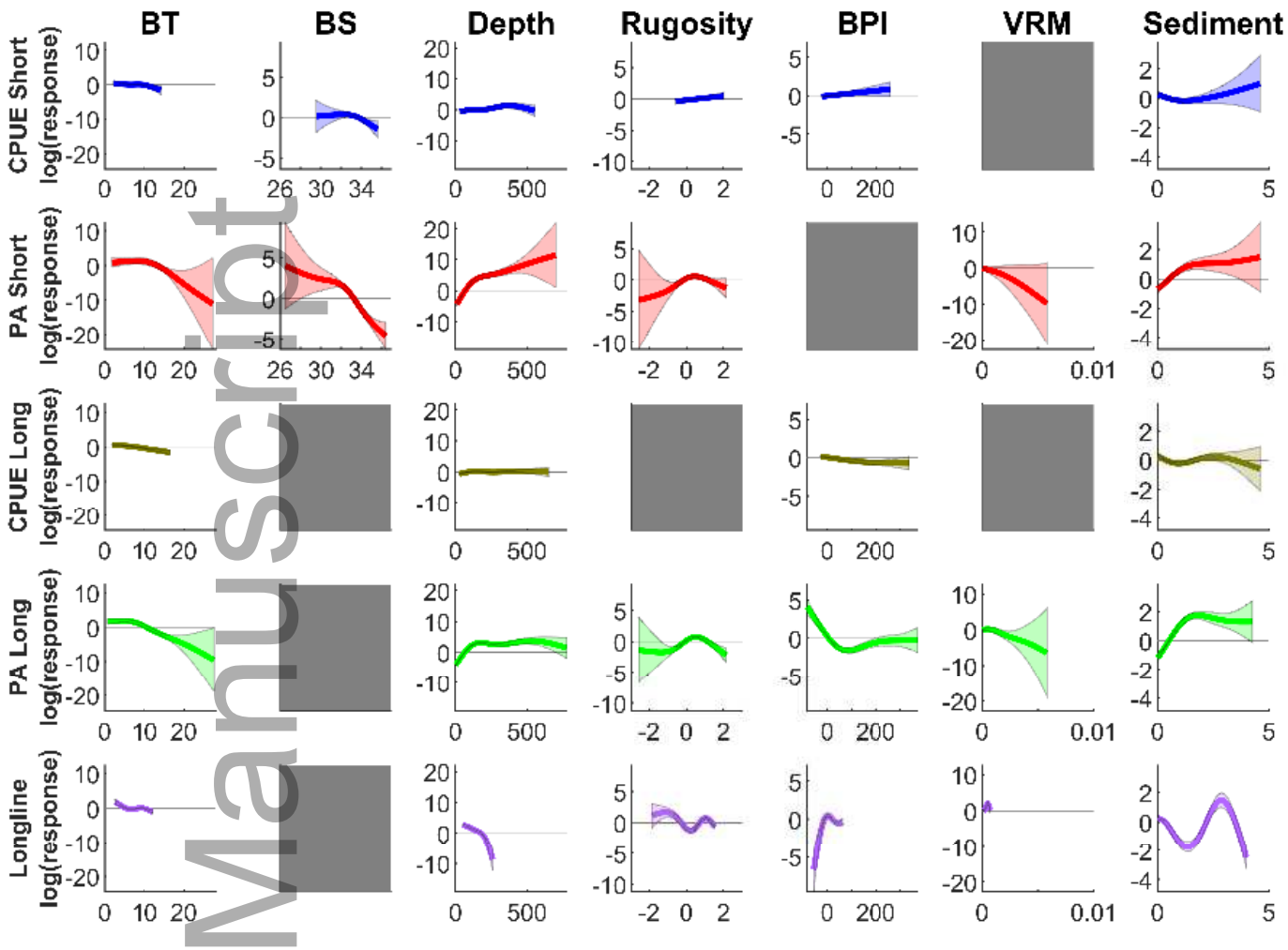


fog_12520_f4.eps

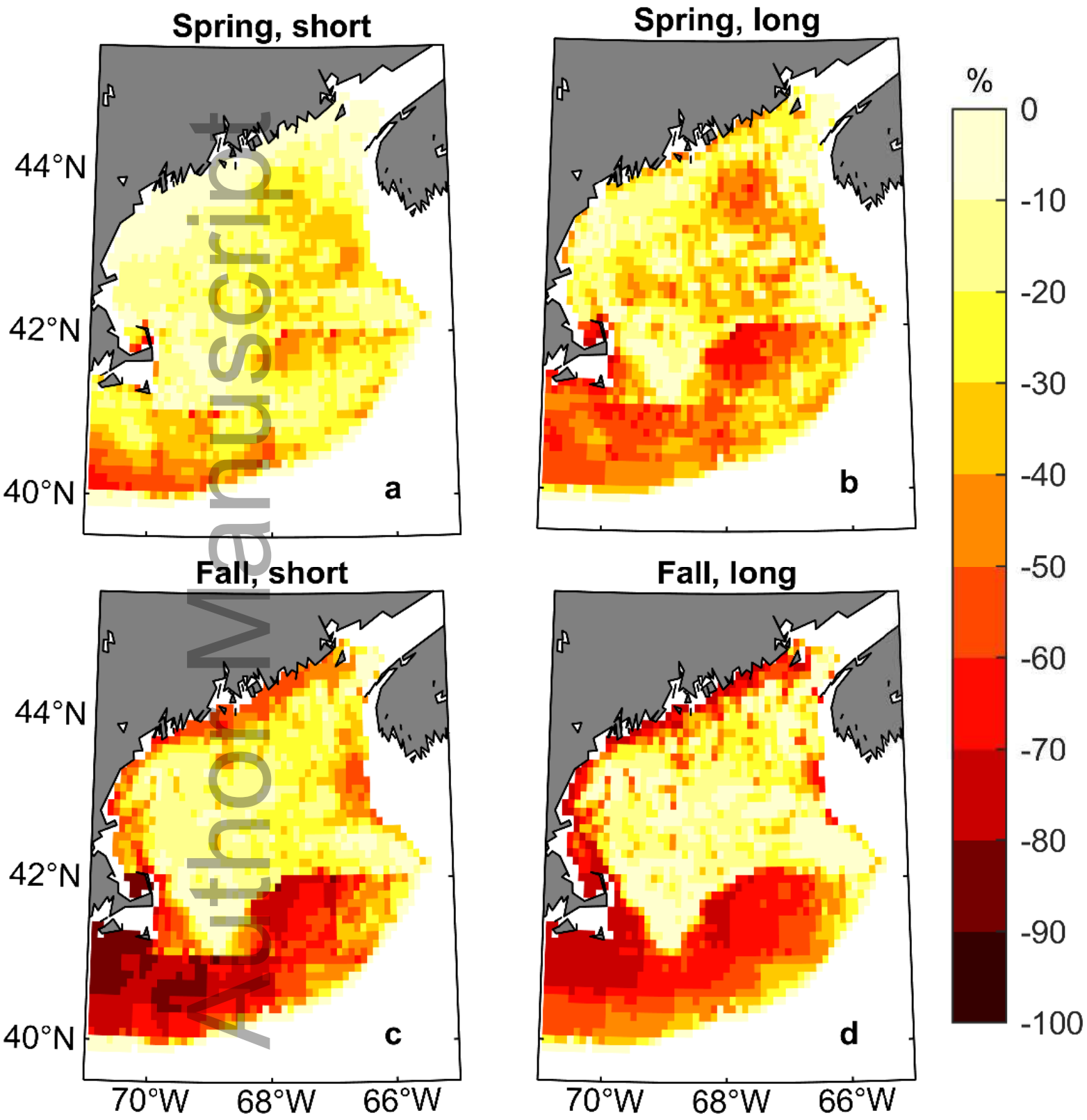




fog_12520_f5.eps

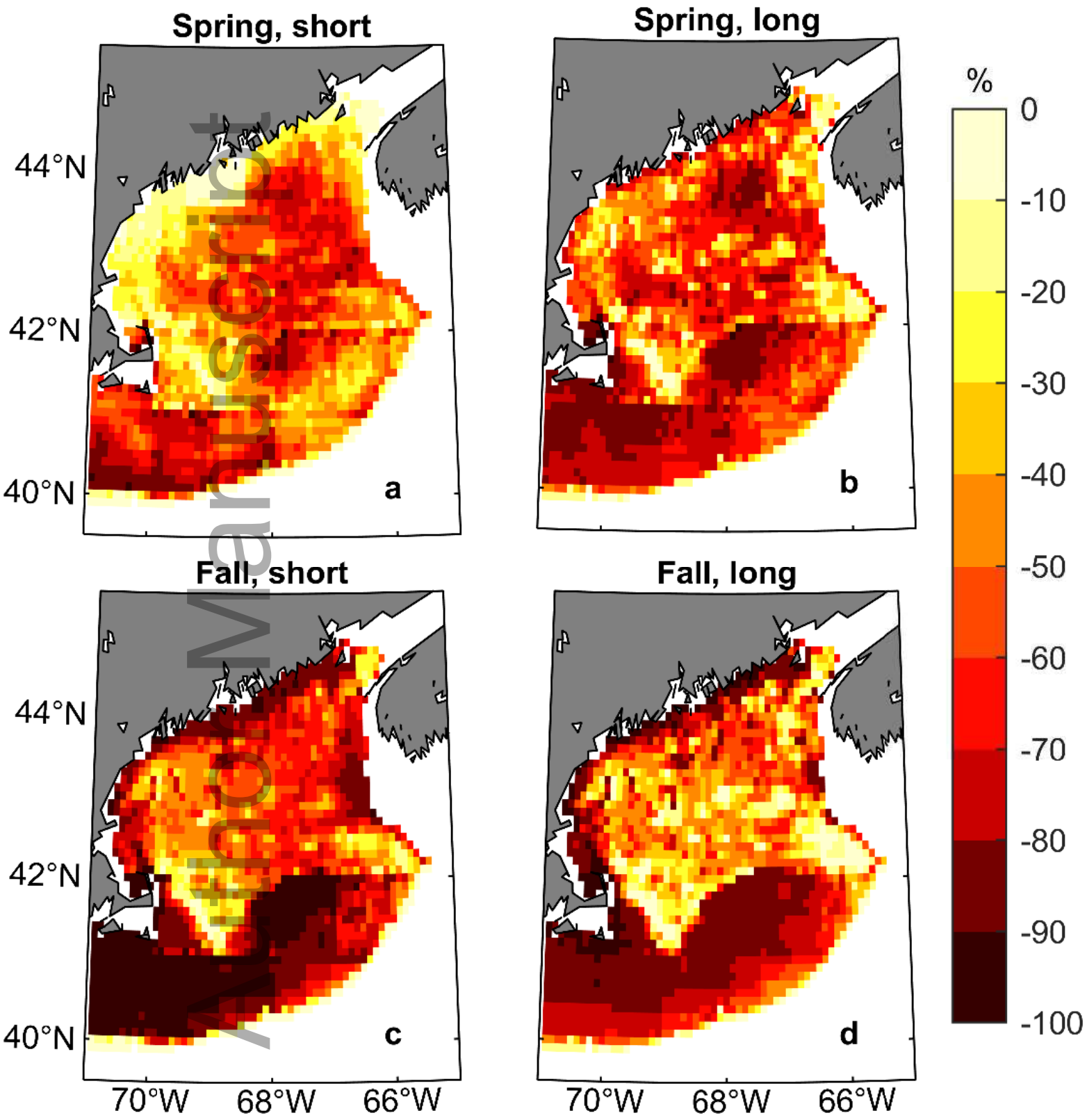




fog_12520_f6.eps

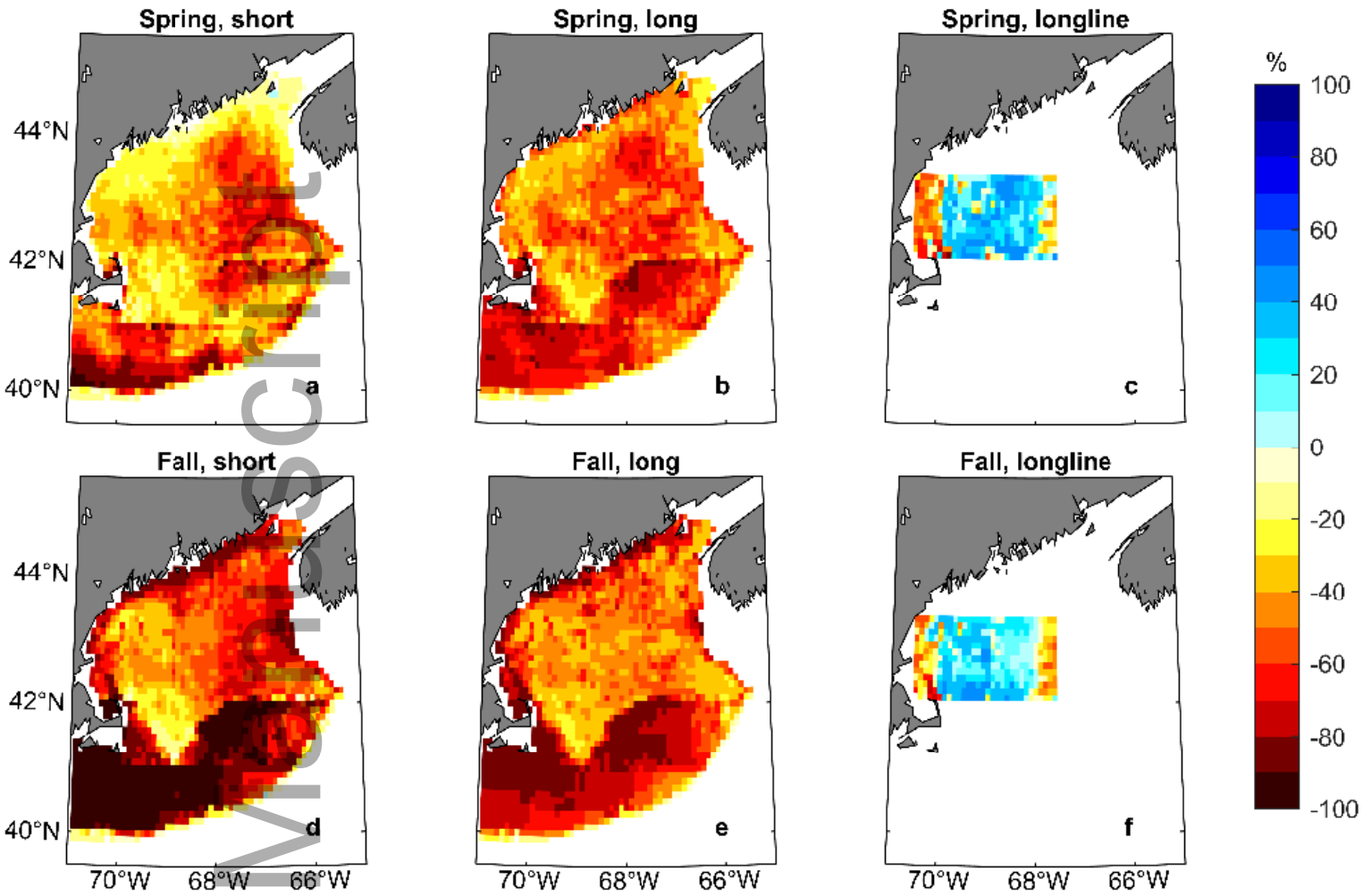


fog_12520_f7.eps

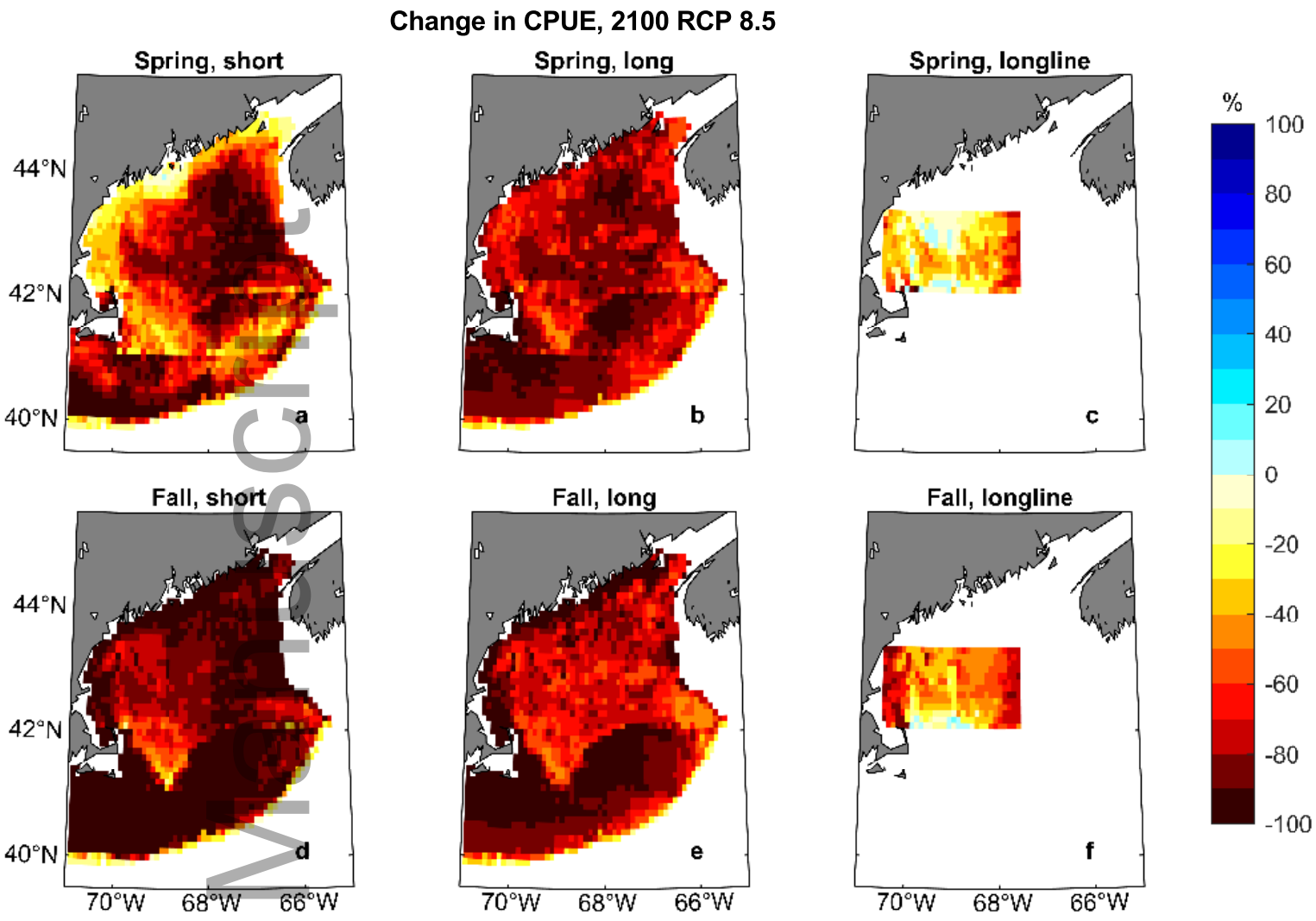


fog_12520_f8.eps

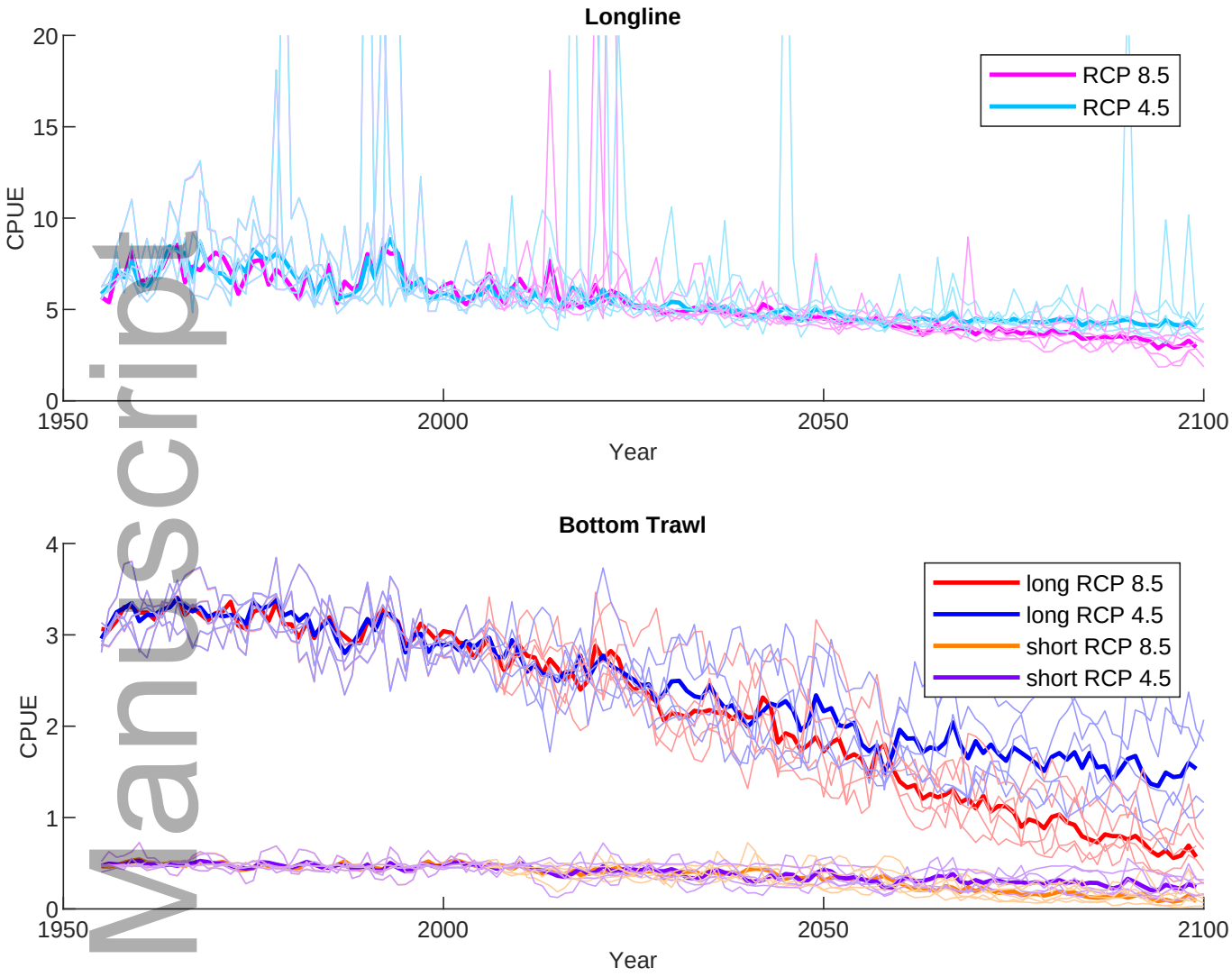


fog_12520_f9.eps